New Journal of Physics
The open access journal at the forefront of physics

Deutsche Physikalische Gesellschaft DPG
IOP Institute of Physics

Published in partnership with: Deutsche Physikalische Gesellschaft and the Institute of Physics

OPEN ACCESS

RECEIVED
9 March 2022

ACCEPTED FOR PUBLICATION
1 April 2022

PUBLISHED
5 May 2022

PAPER

Triple-vortex bremsstrahlung

W Q Wang[1,2], S H Lei[1,2], X S Geng[1], B F Shen[3], Z G Bu[1,*] and L L Ji[1,*]

[1] State Key Laboratory of High Field Laser Physics and CAS Center for Excellence in Ultra-intense Laser Science, Shanghai Institute of Optics and Fine Mechanics (SIOM), Chinese Academy of Sciences (CAS), Shanghai 201800, People's Republic of China
[2] Center of Materials Science and Optoelectronics Engineering, University of Chinese Academy of Sciences, Beijing 100049, People's Republic of China
[3] Shanghai Normal University, Shanghai 200234, People's Republic of China
[*] Authors to whom any correspondence should be addressed.

E-mail: zhigang.bu@siom.ac.cn and jill@siom.ac.cn

Keywords: vortex state, bremsstrahlung, QED scattering, twisted gamma photon

Abstract

Particles in vortex states have gained arising interests due to the additional degree of freedom—the orbital angular momentum (OAM) inherently existing in the state. With the increasing energy of vortex particles (photons, leptons etc), the research has gradually transitioned from the classical field regime to collisions of vortex particles in the quantum-field regime. The latter provides a new way to study the rich properties of particle physics. Here, we show the characteristics of vortex states in bremsstrahlung by deriving the corresponding scattering probability following the quantum-electrodynamics theory. The theory allows us to obtain the OAM distribution of the outgoing vortex photon and the law of OAM transfer during interaction. It is shown that the generated photon takes most of the initial electron OAM, especially when the latter is more energetic. The opening angle of outgoing particles in vortex bremsstrahlung is also significantly different from plane wave scattering. The effects of polarization and non-zero impact parameter are also discussed. The results illustrate the unique feature of vortex scattering and suggest a feasible way to generate high-energy vortex photons—a novel source in studying nuclear physics.

1. Introduction

Beams of photons (vortex light) with nonzero projections of orbital angular momenta (OAM) have been developed for more than 30 years since it was firstly proposed [1]. It is later discovered that not only photons but other particles, such as electrons, also have the vortex feature [2, 3]. Both vortex photons and vortex electrons contain an additional degree of freedom-the orbital-angular-momentum, which brings new effects in various physical processes and sequential applications.

Arising interests have been seen in studies of the properties of these quantum vortex states. The vortex structures under Lorentz transformation have been revealed [4] and the quantization approaches of vortex states were detailed discussed [5]. Moreover, the vortex structure behaves in external magnetic field was revealed, which shows Landau energy levels in condensed matter [6, 7] and the Larmor and Gouy rotations [8]. For relativistic vortex particles, the consistent wave-packet description in paraxial and non-paraxial cases were developed [9–13]. Inclusion of the vortex feature have shown interesting effects in various quantum electrodynamics (QED) processes, such as two-photon annihilation of vortex positrons and Compton scattering of a vortex photon [14, 15].

Preparation of optical vortex beams carrying OAM has been realized using phase plates or diffraction holography in the laboratory [16–23]. And the radiation processes are explored to generate vortex photons at terahertz (THz) frequencies like Smith–Purcell radiation generated by a vortex electron from an conducting diffraction grating [24]. Some material related generation methods from charged particles moving in cholesterics have also been studied as a pure source of twisted photons [25, 26]. However, these mainly concern low energy photons. In the x-ray regime, several schemes based on undulators and wigglers

are proposed to generate vortex x-ray beams from twisted electrons [27, 27–31]. In the higher energy range of gamma-rays, an efficient way is proposed by scattering off relativistic partially stripped ions [32, 33].

Vortex electrons of relativistic energies have shown unique features in the two-particle scattering [34]. The vortex structure in such process is of interest. The presence of OAM is promising in providing new insights in QED realm, which is usually carried out with particles in the plane wave (PW) states. The concept of vortex or twisted scattering enables us to perform experiments on various combinations, such as V (vortex state) + PW (plane wave state) → PW + PW [35–38], V + V → PW + PW [39–45], V + PW → V + PW [46–48], V + PW → V + V [49]. For the scattering processes in which all the final states are PW states, the total angular momentum (TAM) may not be retrieved because the outgoing PW states do not carry the OAM information. When single vortex state is applied before and after the interaction V + PW → V + PW, it is obvious that the OAM of the outgoing vortex particle comes from that of the incident vortex one [46], and the TAM conservation is satisfied. When the interaction involves at least one vortex particle initially, the scattering naturally leads to two vortex-entangled outgoing beams such that all final states should be considered in vortex modes [49]. In other words, the features can not be fully revealed when the out-going particles are only partially described by vortex states.

In this paper, we calculate the bremsstrahlung process where a vortex electron collides with lead nuclei and emit one photon. We describe the outgoing electron and photon in vortex mode and obtain the radiation probability as a function of the OAM projection (V + Z → V + V). Compared with PW scattering, the triple-vortex bremsstrahlung shows opening angles of the final vortex particles highly dependent on the one of the incident electron. We also examined the OAM allocation after the collision. It is found that most of the OAM of the incident electron is transferred to the outgoing vortex photon rather than the electron. This makes it possible to generate high-energy photons with a specific range of OAM through triple-vortex bremsstrahlung. Finally, the influence of the non-zero impact parameter is considered which is of more guiding significance for future experiments.

2. Description of vortex states

We employ the Bessel mode for vortex particle states. It can be constructed by superposing PW states [47] $A^{j,\lambda;\mu}_{k_\perp,k_z}(x) = \int \tilde{A}_j(k'_\perp) A^{\lambda;\mu}_{k'_\perp,k_z}(x) k'_\perp \, \mathrm{d}k'_\perp \, \mathrm{d}\phi_{k'}$, in cylindrical momentum space $k' = (k'_\perp, \phi_{k'}, k'_z)$. Suppose that the vortex photon propagates along the z-axis, j is an eigenvalue of a projection of the TAM operator on z-axis. $\lambda = \pm 1$ represents the helicity of the vortex photon. k_z and $k_\perp = \sqrt{\omega^2 - k_z^2}$ are the photon momentum parallel and perpendicular to z-axis (ω is the photon energy), respectively. Here $A^{\lambda;\mu}_k(x) = \frac{\epsilon^{\lambda;\mu}_k}{\sqrt{(2\pi)^3(2\omega)}} \mathrm{e}^{-\mathrm{i}kx}$ is the PW photon state, $\tilde{A}_j(k'_\perp) = \frac{1}{\sqrt{2\pi}\mathrm{i}^j k'_\perp} \delta(k'_\perp - k_\perp) \mathrm{e}^{\mathrm{i}j\phi_{k'}}$ is the corresponding Fourier spectrum. So, the vortex photon state can be expressed as:

$$
\begin{aligned}
A^{j,\lambda;\mu}_{k_\perp,k_z}(x) &= \epsilon^{j,\lambda;\mu}_{k_\perp,k_z}(\boldsymbol{r}) \mathrm{e}^{\mathrm{i}k_z z - \mathrm{i}\omega t} \\
&= \frac{\mathrm{e}^{\mathrm{i}k_z z - \mathrm{i}\omega t}}{4\pi\sqrt{\omega}} \begin{pmatrix} 0 \\ \left(\frac{\mathrm{i}}{2}\right)\left[\left(1 - \frac{k_z}{\omega}\right)\Theta^{j+\lambda}_{k_\perp}(\boldsymbol{r}) + \left(1 + \frac{k_z}{\omega}\right)\Theta^{j-\lambda}_{k_\perp}(\boldsymbol{r})\right] \\ \left(\frac{\lambda}{2}\right)\left[\left(1 - \frac{k_z}{\omega}\right)\Theta^{j+\lambda}_{k_\perp}(\boldsymbol{r}) - \left(1 + \frac{k_z}{\omega}\right)\Theta^{j-\lambda}_{k_\perp}(\boldsymbol{r})\right] \\ \left(\frac{\lambda k_\perp}{\omega}\right)\Theta^{j}_{k_\perp}(\boldsymbol{r}) \end{pmatrix},
\end{aligned} \tag{1}
$$

where $\epsilon^{j,\lambda;\mu}_{k_\perp,k_z}(\boldsymbol{r})$ represents the polarization vector and the transverse function is defined by $\Theta^n_{k_\perp}(\boldsymbol{r}) = J_n(k_\perp r) e^{in\theta}$ ($J_n(r)$ is the first kind of Bessel function).

Similarly, for electrons, the vortex states can also be written as superposition of PW states, which is $\psi^{m,s}(x) = \int \tilde{\psi}_m(p'_\perp) \psi(x) p'_\perp \, \mathrm{d}p'_\perp \, \mathrm{d}\phi$. The PW state of electron is $\psi(x) = \frac{1}{\sqrt{2(2\pi)^3}} \mathrm{e}^{-\mathrm{i}px}(\sqrt{1 + \frac{M}{E}}\xi^s, \sqrt{1 - \frac{M}{E}}(\boldsymbol{\sigma}\cdot\boldsymbol{\kappa})\xi^s)$. Fourier spectrum of electron is $\tilde{\psi}_m(p'_\perp) = \frac{1}{\sqrt{2\pi}\mathrm{i}^m p'_\perp} \delta(p'_\perp - p_\perp) \mathrm{e}^{\mathrm{i}m\phi_{p'}}$. The unit momentum vector along the momentum direction is defined as $\boldsymbol{\kappa} = \boldsymbol{p}/|\boldsymbol{p}|$ and p_z and $p_\perp = \sqrt{E^2 - M^2 - p_z^2}$ are the z-component and perpendicular one of the electron momentum. Here E is energy and M is the rest mass of the vortex electron. m is a number related to the OAM projection of the vortex electron on z-axis [42], $s = \pm 1$ is the vortex electron helicity. Hence, we have

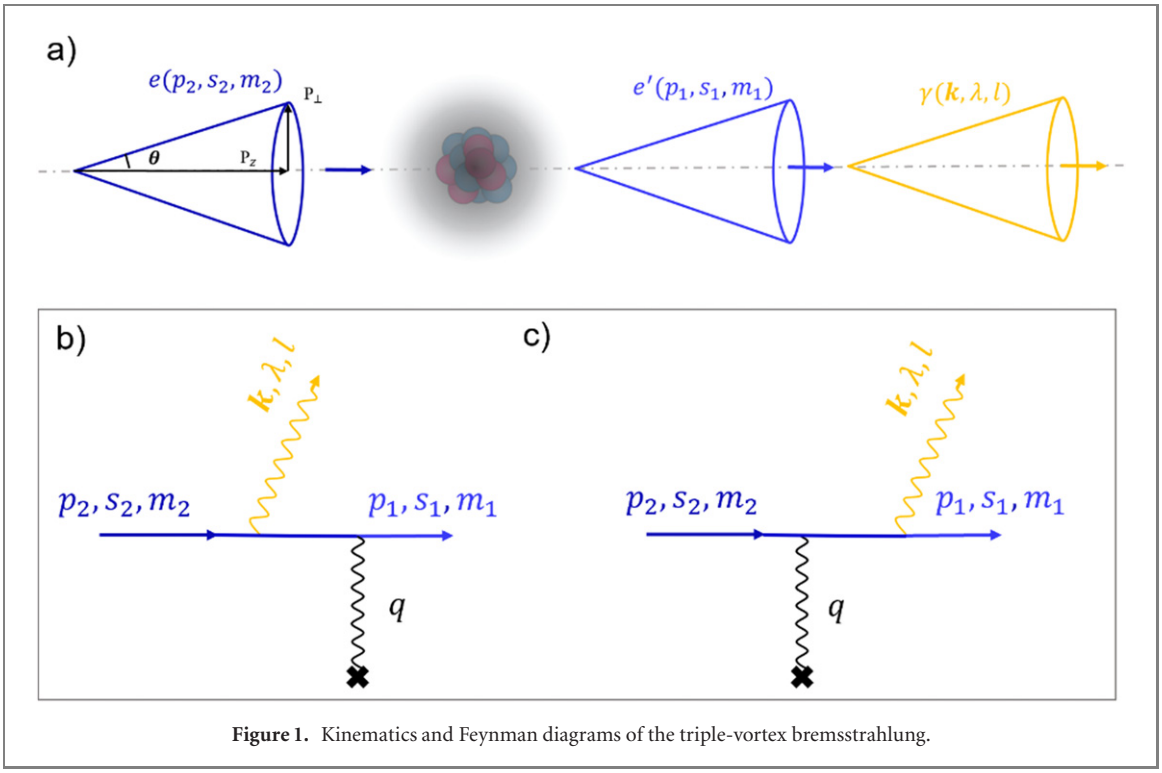

Figure 1. Kinematics and Feynman diagrams of the triple-vortex bremsstrahlung.

the vortex electron wave function propagating along the z-axis:

$$\begin{aligned}\psi^{m,s}_{p_\perp,p_z}(x) &= u^{m,s}_{p_\perp,p_z}(r,\theta)\mathrm{e}^{\mathrm{i}p_z z-\mathrm{i}Et}\\ &= \frac{\mathrm{e}^{\mathrm{i}p_z z-\mathrm{i}Et}}{\sqrt{2}(2\pi)}\frac{1}{|p|}\sqrt{1-\frac{M}{E}}\left[\begin{pmatrix}(E+M)\xi^s\\ p_z\sigma_z\xi^s\end{pmatrix}\Theta^m_{p_\perp}(r)+\mathrm{i}p_\perp\begin{pmatrix}0\\ \sigma^{\perp,m}_{p_\perp}(r,\theta)\xi^s\end{pmatrix}\right],\end{aligned} \tag{2}$$

where the transversal matrix reads $\sigma^{\perp,m}_{p_\perp}(r,\theta)=\begin{bmatrix}0 & -\Theta^{m-1}_{p_\perp}(r)\\ \Theta^{m+1}_{p_\perp}(r) & 0\end{bmatrix}$. The orthogonality and normalization of the wave functions of photon and electron as defined above is shown in appendix A.

We focus on the distinctive properties between the vortex states and PW states. For vortex states we employ the projection formalism following the one discussed in [5]. So these physical quantities can be studied in experiments, where vortex properties for low energy particles have been measured [7]. Here neither spin quantum number nor angular quantum number are the eigenvalues of their corresponding operators $\hat{S}$ and $\hat{L}$, and only their sum j (TAM) is the eigenvalue of TAM operator $\hat{J}$ [50]. It is worth mentioning that TAM of vortex photon is included in the transverse function, while for the vortex electron the OAM values are not only seen in the vortex function, but also included in the transverse matrix composed of transverse functions, because they are spinors rather than vectors. The OAM dimension of vortex states can interact with other physical quantities to realize the phenomenon that cannot be observed in PW states, and then explore potential noval applications. For example, the interaction between the OAM and magnetic lenses exhibits Larmor and Gouy rotations [8].

3. Theoretical description of triple-vortex bremsstrahlung

In this paper, the forward and backward scatterings are discussed, and the average momenta of particles are parallel to z-axis, as shown in figure 1(a). Here a vortex electron collides with a stationary bare lead nucleus to produce vortex electron and photon. Therefore, the axis of the helicity is also along z-axis. In this way, the TAM projection and helicity can be described along the same z-axis. To discuss the properties of photon OAM that is not well defined in wave function, we define a parameter $l = j - \lambda$. Based on this definition, l is closely associated with the photon OAM, but not equivalent to the physical definition of photon OAM. Furthermore, it should be noted that only the projection of TAM operator on some axis has the well defined eigen value j. For photon, j is independent of λ; for electron $j = m + s/2$. $c = \hbar = 1$ is used in the derivation.

According to QED, the S-matrix element of triple-vortex bremsstrahlung is as follows:

$$\begin{aligned} S_{fi} &= S_1 + S_2 \\ &= -ie^2 \int d^4x\, d^4y\, \overline{\psi_1}(x)[\gamma^\mu A^*_\mu(x) S_F(x-y)\gamma^0 A_0(y) + \gamma^0 A_0(x) S_F(x-y)\gamma^\nu A^*_\nu(y)]\psi_2(y). \end{aligned} \tag{3}$$

S_1 and S_2 represent two Feynman diagrams of bremsstrahlung shown in figures 1(b) and (c) respectively.

The physical quantities of outgoing and incident electrons are marked with subscripts 1 and 2 respectively, and p represents the momentum of intermediate propagator. The electron propagator is defined as: $S_F(x-y) = \int \frac{d^4p}{(2\pi)^4} \frac{\gamma_\mu p^\mu + M}{p^2 - M^2} e^{-ip(x-y)}$ and $A_0 = -\frac{Ze}{4\pi|\vec{x}|} = -Ze \int \frac{d^3q}{(2\pi)^3} \frac{1}{|\vec{q}|^2} e^{i\vec{q}\cdot\vec{x}}$ is the Coulomb field of the nucleus (for lead nucleus, $Z = 82$).

Substituting equations (1) and (2) into equation (3) and transforming them into cylindrical coordinate system, we obtain the following results

$$S_{f\,i} = \frac{-iZe^3}{32\pi^3} \delta(E_1 + \omega - E_2) \frac{1}{|\vec{p_1}||\vec{p_2}|} \sqrt{\frac{(E_1 - M)(E_2 - M)}{\omega E_1 E_2}} \cdot \xi^{s_1\dagger}(\Sigma_1 + \Sigma_2)\xi^{S_2}, \tag{4}$$

where:

$$\Sigma_1 = \int dp_\perp\, dq_\perp\, p_\perp q_\perp \frac{1}{p^2 - M^2} \frac{1}{|\vec{q}|^2} \Xi_1, \tag{5}$$

$$\Sigma_2 = \int dp_\perp\, dq_\perp\, p_\perp q_\perp \frac{1}{p^2 - M^2} \frac{1}{|\vec{q}|^2} \Xi_2. \tag{6}$$

Matrix $\Xi_1 + \Xi_2$ takes the following form:

$$\Xi_1 + \Xi_2 = \begin{bmatrix} A\delta_{m_2,m_1+j} & B\delta_{m_2,m_1+j+1} \\ C\delta_{m_2,m_1+j-1} & D\delta_{m_2,m_1+j} \end{bmatrix}. \tag{7}$$

where A, B, C and D are the coefficients of the four matrix elements (the complete derivation is shown in appendix B), and the four Kronecker symbols define the TAM conservation in different spin cases. Next, we illustrate how conservation of angular momentum is dependent on the particle spin. While both the incident and the outgoing electron spins are up: $\xi^{s_2} = \begin{bmatrix} 1 \\ 0 \end{bmatrix}, \xi^{s_1} = \begin{bmatrix} 1 \\ 0 \end{bmatrix}$, the relationship given by the conservation law of TAM is $\delta((m_2 + \frac{1}{2}) - (m_1 + \frac{1}{2}) - j) = \delta(m_2 - m_1 - j)$, the corresponding term is $A\delta_{m_2,m_1+j}$; while the incident electron spin is down and the outgoing one is up: $\xi^{s_2} = \begin{bmatrix} 0 \\ 1 \end{bmatrix}, \xi^{s_1} = \begin{bmatrix} 1 \\ 0 \end{bmatrix}$ the conservation law gives $\delta((m_2 - \frac{1}{2}) - (m_1 + \frac{1}{2}) - j) = \delta(m_2 - m_1 - j - 1)$, which is seen from the term $B\delta_{m_2,m_1+j+1}$. The other two cases can be verified accordingly. It can be seen that the equation (7) of triple-vortex bremsstrahlung is fully self-consistent with the conservation law of TAM.

The four Kronecker symbols also show the constraint relation of the angular momentum of the triple-vortex structures in which three particles combine when the single-vortex structures of the free particle are discussed in [4]. Such constraint relation indicates the entanglement between angular momentum of final particles and new effects emerge when vortex structures are exposed to an external field like a magnetic field [6]. In this paper, the role of nucleus is equivalent to creating a spherically symmetric electric field.

We use wave packets to describe incident electron:

$$\psi_{\text{wave-packet}}(x) = \int \frac{dp_z\, dp_\perp p_\perp}{\sqrt{2E}} \rho(p_\perp, p_z) \psi^{m,s}_{p_\perp,p_z}(x), \tag{8}$$

with normalization:

$$\int \frac{dp_z\, dp_\perp\, p_\perp}{2E} |\rho(p_\perp, p_z)|^2 = 1. \tag{9}$$

We assume that $\rho(p_\perp, p_z) = N_{\tau_\perp,\tau_z} \exp[-\frac{(p_\perp - \tilde{p}_\perp)^2}{\tau_\perp^2} - \frac{(p_z - \tilde{p}_z)^2}{\tau_z^2}]$ and $\tau_\perp(z) \ll \tilde{p}_\perp(z)$. According to equation (9), one has

$$N^2_{\tau_\perp,\tau_z} = \frac{2E}{\sqrt{\frac{\pi}{2}}\tau_z \left(\frac{\tau_\perp^2}{4} + \frac{\tilde{p}_\perp \tau_\perp}{2} \sqrt{\frac{\pi}{2}} \left(1 - \text{erf}\left(\frac{-2\tilde{p}_\perp}{\sqrt{2}\tau_\perp}\right)\right)\right)}. \tag{10}$$

By substituting the wave function equation (8) into the S-matrix element, we get

$$S_{\text{wave-packet}} = \int \frac{\mathrm{d}p_{2z}\,\mathrm{d}p_{2\perp}\,p_{2\perp}}{\sqrt{2E_2}}\rho(p_{2\perp},p_{2z})\delta(E_2-\omega-E_1)S_{fi}, \tag{11}$$

where we take δ function out of S_{fi}. According to Fermi's golden rules, the scattering probability of triple-vortex bremsstrahlung is as follows:

$$\mathrm{d}P = k_\perp p_{1\perp}|S_{\text{wave-packet}}|^2\,\mathrm{d}k_\perp\,\mathrm{d}k_z\,\mathrm{d}p_{1\perp}\,\mathrm{d}p_{1z}. \tag{12}$$

The probability can also be viewed in the energy-angular domain by replacing the momenta via $E^2 = M^2 + p_\perp^2 + p_z^2$ ($\omega^2 = k_\perp^2 + k_z^2$ for photon):

$$\mathrm{d}P = k_\perp p_{1\perp}|S_{\text{wave-packet}}|^2\omega\,\mathrm{d}\omega\,\mathrm{d}\theta_k E_1\,\mathrm{d}E_1\mathrm{d}\theta_1, \tag{13}$$

where θ_k and θ_1 are the opening angles of outgoing photon and electron following $k_\perp = \omega\,\sin\,\theta_k, k_z = \omega\,\cos\,\theta_k; p_{1\perp} = \sqrt{E_1^2 - M^2}\,\sin\,\theta_1, p_{1z} = \sqrt{E_1^2 - M^2}\,\cos\,\theta_1$.

Integrating $\mathrm{d}E_1$ by using $\delta(E_2 - E_1 - \omega)$ which is contributed by $|S_{\text{wave-packet}}|^2$, the differential scattering probability of triple-vortex bremsstrahlung is finally obtained:

$$\frac{\mathrm{d}P}{\mathrm{d}\omega\,\mathrm{d}\theta_k\,\mathrm{d}\theta_1} = k_\perp p_{1\perp}\omega E_1|S_{\text{wave-packet}}|^2|_{E_1=E_2-\omega}. \tag{14}$$

It is worth noting that in the calculation of scattering probability, there are one delta function and four Kronecker symbols, which represent the total energy conservation and the TAM conservation for triple vortex bremsstrahlung. In PW bremsstrahlung, there is only one delta function defining the conservation of energy. Because the PW particles do not carry OAM, the scattering cross section does not contain related information.

Our above derivation assumes that the incident electron strikes the center of the nucleus along the z-axis (impact parameter $b = 0$). However, there is often a certain deviation from the z-axis in experiments. The effects of impact parameter b need to be considered. The incident electron wave function with a b ($\vec{b} = (b_x, b_y, 0)$, $b = |\vec{b}|$, $\cos\theta_b = b_x/b$) distance offset from the z axis has the following form (see appendix C for the specific derivation):

$$\begin{aligned}\psi^{s_2}_{p_2,m_2}(x,\vec{b}) &= \int \tilde{\psi}_{m_2}(\vec{p'})\psi(x)\mathrm{e}^{-\mathrm{i}\vec{p'}_\perp\cdot\vec{b}}p'_\perp\,\mathrm{d}p'_\perp\,\mathrm{d}\phi_{p'}\,\mathrm{d}p'_z \\ &= \sum_n \mathrm{e}^{-\mathrm{i}n\theta_b}J_n(p_{2\perp}b)\cdot\psi^{s_2}_{p_2,m'_2}(x)|_{m'_2=m_2+n}.\end{aligned} \tag{15}$$

Bring equation (15) into the above derivation process to obtain the scattering amplitude considering the impact distance:

$$S_{\text{wave-packet}}(\vec{b}) = \sum_n \mathrm{e}^{-\mathrm{i}n\theta_b}J_n(p_{2\perp}b)\cdot S_{\text{wave-packet}}|_{m_2\to m'_2, m'_2=m_2+n}. \tag{16}$$

The differential scattering probability can be written as follows:

$$\frac{\mathrm{d}P(\vec{b})}{\mathrm{d}\omega\,\mathrm{d}\theta_k\,\mathrm{d}\theta_1} = k_\perp p_{1\perp}\omega E_1|S_{\text{wave-packet}}(\vec{b})|^2|_{E_1=E_2-\omega}. \tag{17}$$

The norm square is calculated as follows:

$$\begin{aligned}\int \mathrm{d}\theta_b|\sum_n \mathrm{e}^{-\mathrm{i}n\theta_b}J_n(p_{2\perp}b)|^2 &= \int \mathrm{d}\theta_b\sum_{n,n'}\mathrm{e}^{-\mathrm{i}(n-n')\theta_b}J_n(p_{2\perp}b)J_{n'}(p_{2\perp}b) \\ &= \sum_{n,n'}\delta_{n,n'}J_n(p_{2\perp}b)J_{n'}(p_{2\perp}b) \\ &= \sum_n J_n^2(p_{2\perp}b).\end{aligned} \tag{18}$$

Finally, we obtain the differential scattering probability with impact distance b:

$$\frac{\mathrm{d}P(\vec{b})}{\mathrm{d}\omega\,\mathrm{d}\theta_k\,\mathrm{d}\theta_1} = k_\perp p_{1\perp}\omega E_1 \sum_n J_n^2(p_{2\perp}b)|S_{\mathrm{wave-packet}}|^2|_{E_1=E_2-\omega,m_2\to m_2',m_2'=m_2+n}$$
$$= \sum_n J_n^2(p_{2\perp}b)\frac{\mathrm{d}P}{\mathrm{d}\omega\,\mathrm{d}\theta_k\,\mathrm{d}\theta_1}|_{m_2\to m_2',m_2'=m_2+n}. \tag{19}$$

Equation (19) shows that the scattering probability with a non-zero impact parameter is the weighted superposition of the scattering probabilities of incident electrons with different m_2 and a impact parameter of 0. This weight is $J_n^2(p_{2\perp}b)$. When b is constant and $p_{2\perp}b$ is constant, the characteristic of Bessel function indicates that when the independent variable is fixed and n exceeds a certain threshold, the function value tends to 0, then the weight tends to 0, so the final summation result is a convergent value. When we consider colliding with a macroscopic target, we need to integrate b to obtain an averaged scattering probability:

$$\frac{\mathrm{d}\bar{P}}{\mathrm{d}\omega\,\mathrm{d}\theta_k\,\mathrm{d}\theta_1} = \int \mathrm{d}b\frac{\mathrm{d}P(\vec{b})}{\mathrm{d}\omega\,\mathrm{d}\theta_k\,\mathrm{d}\theta_1}$$
$$= \sum_n \int \mathrm{d}b J_n^2(p_{2\perp}b)\frac{\mathrm{d}P}{\mathrm{d}\omega\,\mathrm{d}\theta_k\,\mathrm{d}\theta_1}|_{m_2\to m_2',m_2'=m_2+n}, \tag{20}$$

which means that the averaged scattering probability is equivalent to the modification of the weight by integrating b.

4. Numerical results and discussion

In the last chapter, we have obtained the differential scattering probability of triple-vortex bremsstrahlung. We consider the incident vortex electron of energy 5 MeV, 10 MeV, 20 MeV and OAM projection $m_2 = 5$. The incident electron wave packet parameters are set as $\tau_\perp/p_{2\perp} = 2.5\%, \tau_z/p_{2z} = 4.5\%$. We choose quantities that can be studied in experiments.

4.1. Opening angle distribution of triple-vortex bremsstrahlung

Comparing with PW states, vortex states not only carry the information of OAM, but also exhibit different momentum space structure. The vertical and parallel momentum of vortex states form an opening angle, e.g. $\theta_2, \theta_1, \theta_k$ in figure 1(a). The effects of different incident electron angles on the scattering process are discussed for three opening angles $\theta_2 = 15°, \theta_2 = 30°, \theta_2 = 45°$. The probability distribution as a function of the opening angles for outgoing particles is shown in figure 2 by fixing the photon energy at $\omega = 1$ MeV.

It is obvious from figure 2 that the scattering probability is the largest when the opening angles of both the outgoing vortex photon and electron coincide with that of the incoming vortex electrons. In other words, the angular distributions of final particles are largely defined by the incident vortex electron.

In addition, in figure 2, there is a bright vertical line at the same position of the opening angle of the outgoing vortex photon and that of the incident electron, but the outgoing vortex electron does not have this feature. It can be seen that the outgoing vortex photon is more dependent on the opening angle of the incident electron than the outgoing vortex electron.

At the same time, there is a second slanting bright line with a negative slope. Figures 2(1)–(3) indicate that the slope is dependent on the incident electron energy. With the increase of the incident electron energy, the slope is close to zero. This slope represents an allocation of opening angles between two outgoing particles. When the outgoing electron energy accounts for more of the total energy, the electron tends to get the same opening angle as the incident electron.

These two distributions are essentially two kinds of opening angular distributions dominated by outgoing electron and photon (the vertical bright line is dominated by photon, and the inclined bright line is dominated by electron). It is obvious that the opening angle distribution range of electron is much wider than that of photon. Note that these two distributions have a coincidence point: the highlight in these pictures. Away from this point, the differential probability drops rapidly. That is to say, for triple-vortex bremsstrahlung, the opening angles of outgoing particles can be regarded as equal to those of incident electrons.

4.2. OAM transfer in triple vortex bremsstrahlung

From equation (7) we know that TAM of triple-vortex bremsstrahlung is conserved. After collision with the nucleus, the angular momentum of the incident vortex electron is transferred to the outgoing particles. It

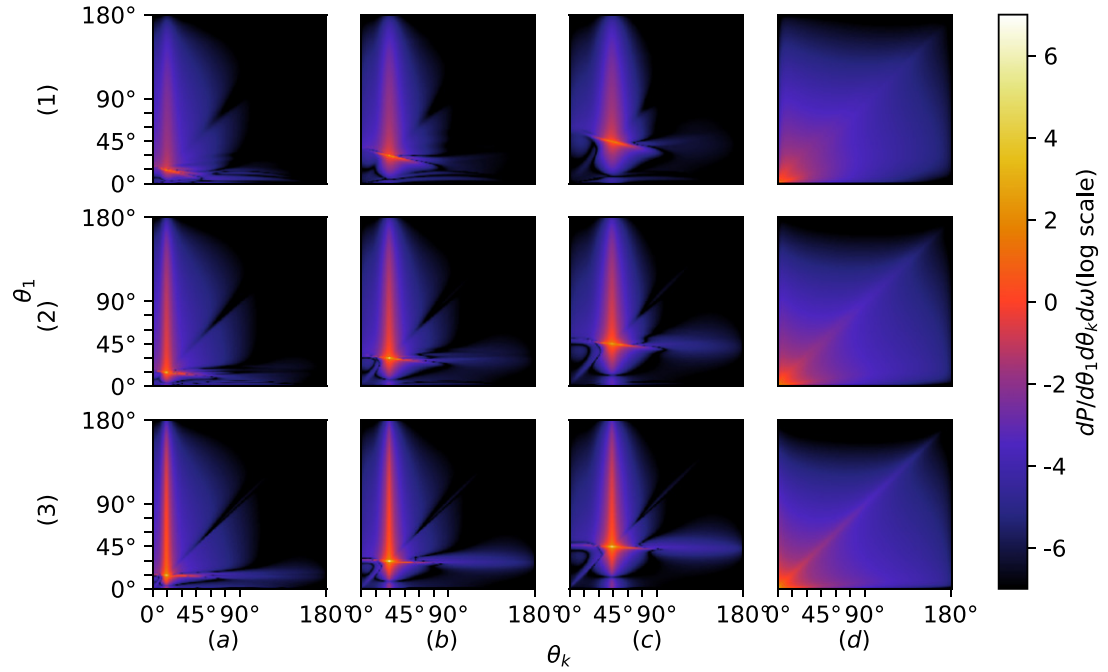

Figure 2. Opening angles—probability distribution. The opening angle of the incident vortex electron is (a) $\theta_2 = 15°$, (b) $\theta_2 = 30°$, (c) $\theta_2 = 45°$. (d) is the PW case. The incident electron energy is (1) $E_2 = 5$ MeV, (2) $E_2 = 10$ MeV, (3) $E_2 = 20$ MeV. the outgoing photon energy is $\omega = 1$ MeV, the spins of the incident electron and the outgoing electron and photon are $\xi^{s_2} = [10]$, $\xi^{s_1} = [10]$, $\lambda = 1$. TAM number of the outgoing photon is $j = 6$.

should be noted that in the triple-vortex bremsstrahlung, after passing through the electrostatic field generated by the nucleus, the two final particles are entangled with each other, which makes the observation of entangled quantities different from that of a single particle. The observation of a particle's entangled quantity will lead to the determination of another one. Since OAMs of the outgoing photon and electron are entangled [49], it is important to find out how the angular momentum is assigned to each of them. Therefore, when we discuss the photon OAM in this paper, the OAM of the electron will automatically be a corresponding determined value due to the collapse of the wave function, and there is no need to integrate like the vortex angle. When the angular momentum of one particle is determined the one of the other particle is also known.

We assume that we have determined the angular momentum of an outgoing photon through detecting, so that OAM of the outgoing photon and the outgoing electron is determined by the conservation of TAM. The distribution of scattering probability with respect to OAM of the outgoing photon is shown in figure 3.

Figure 3 shows that the maximum scattering probability appears in the OAM carried by the outgoing photon equal to the OAM of incident electron. As the photon OAM deviates from the peak position, the scattering probability first decreases rapidly, then decreases slowly by order and becomes stable gradually.

The curves of the three colors in figure 3 show that for different photon energy the curves have the same trend, so that this distribution is independent of the outgoing photon energy. It is worth noting that for 5 MeV, there is a secondary peak between $l = 2$ and $l = 3$ besides the main peak. This is due to the existence of two outgoing particles, which share the OAM of the incident electron. When the incident electron energy is low, there will be a 1:1 distribution trend which leads to asymmetry along $l = 5$. With the increase of energy, the asymmetry decreases at 10 MeV, and is almost symmetrical at 20 MeV, which indicates that the increase of energy will smooth out the asymmetry of OAM distribution according to the number of particles.

For the case of high incident energy ($E_2 = 20$ MeV), the symmetry can be preserved. The symmetry of OAM—probability distribution under spin flip is shown in figure 4. The black dotted line represents the symmetry axis of TAM-probability distribution of the two spin flip processes. We define operators $\widehat{F}_s$ that represents the spin flip transformation of all particles in a scattering process:

$$\widehat{F}_s \, \mathrm{d}\sigma \, \widehat{F}_s^{-1} = \mathrm{d}\sigma|_{\mathrm{spinflip}}, \tag{21}$$

for the scattering probability in this paper: $\widehat{F}_s \mathrm{dProb} \widehat{F}_s^{-1} = \mathrm{dProb}|_{\mathrm{spinflip}}$.

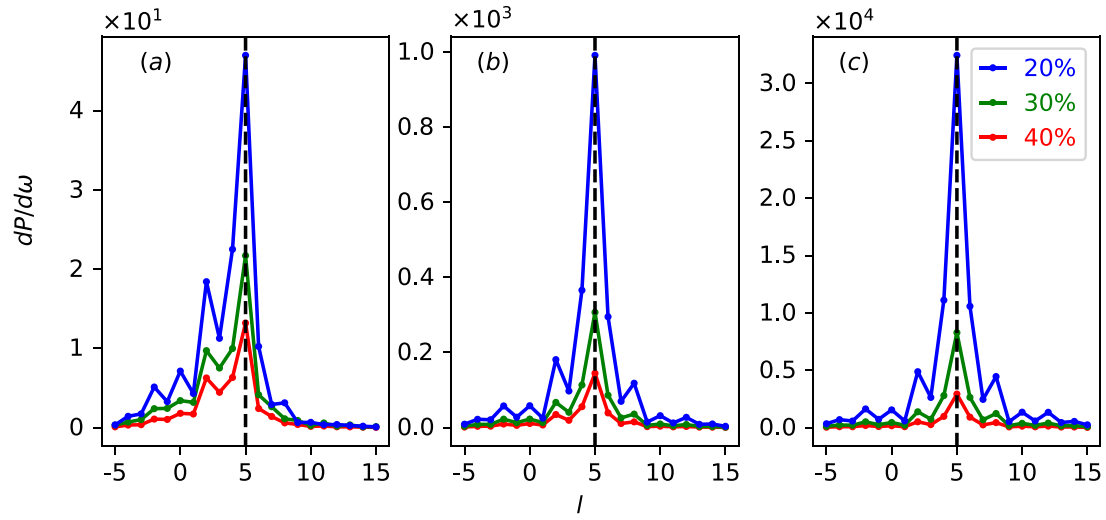

Figure 3. l-probability distribution. (a)–(c) represent energy of the incident electron at $E_2 = 5$ MeV, $E_2 = 10$ MeV, $E_2 = 20$ MeV. $\theta_2 = 30°$, integral range of θ_1 and θ_k is 20°–40°. Three color curves represent $\omega/E_2 = 20\%$, $\omega/E_2 = 30\%$ and $\omega/E_2 = 40\%$, respectively. Spin of the incident electron is averaged, spins of the outgoing electron and photon are summed.

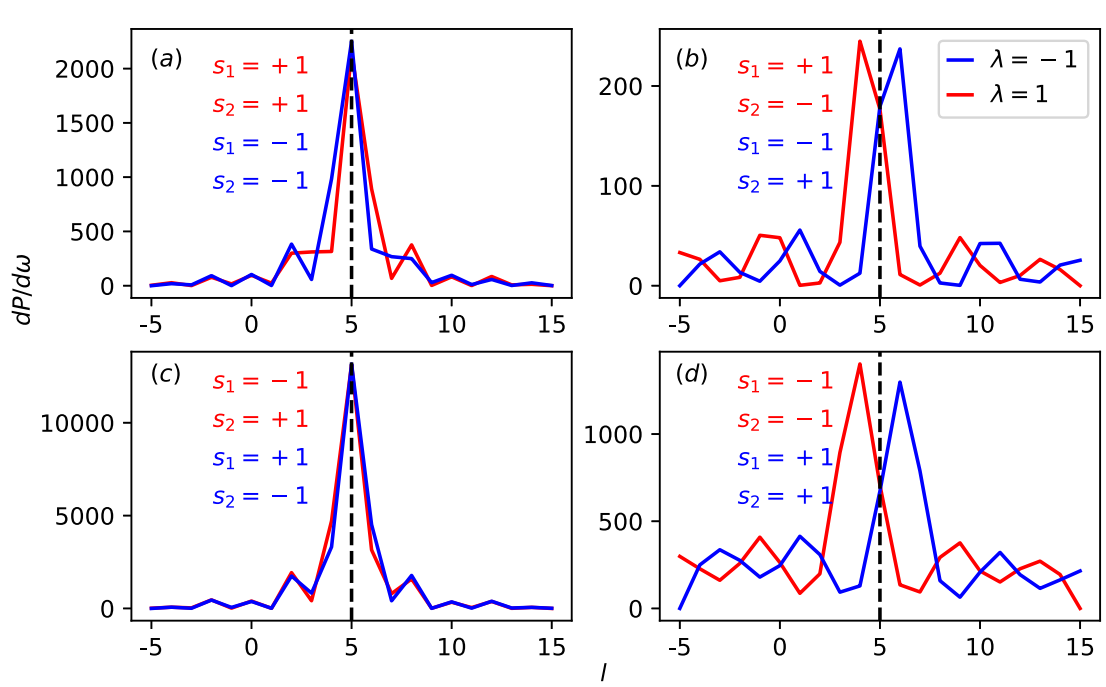

Figure 4. Figures (a)–(d) represent l-probability distributions for different helicity of particles. $E_2 = 20$ MeV, $\omega/E_2 = 20\%$. Blue and red color curves represent $\lambda = -1$ and $\lambda = 1$, respectively.

According to the position of the symmetry axis in figure 4, we obtain the transformation formula of triple-vortex bremsstrahlung under spin flip:

$$\widehat{F}_{\mathrm{s}}\mathrm{dProb}(l)\widehat{F}_{\mathrm{s}}^{-1} = \mathrm{dProb}(2m_2 - l). \tag{22}$$

Equation (22) represents that for triple-vortex bremsstrahlung, if the spins of incident electron, outgoing electron and outgoing photon are all reversed, then the photon OAM—scattering probability distribution will be symmetric along $l = m_2$.

Since the bremsstrahlung process is infrared divergent, we choose specific photon energy in the previous analysis. For different photon energy, whether the OAM distribution characteristics change is also very important. The relationship between the photon average OAM and photon energy in the triple-vortex bremsstrahlung process is shown in figure 5. For figure 5(a) ($E_2 = 5$ MeV), with the increase of photon energy, the average OAM first decreases and then increases. The decrease and increase amplitude become

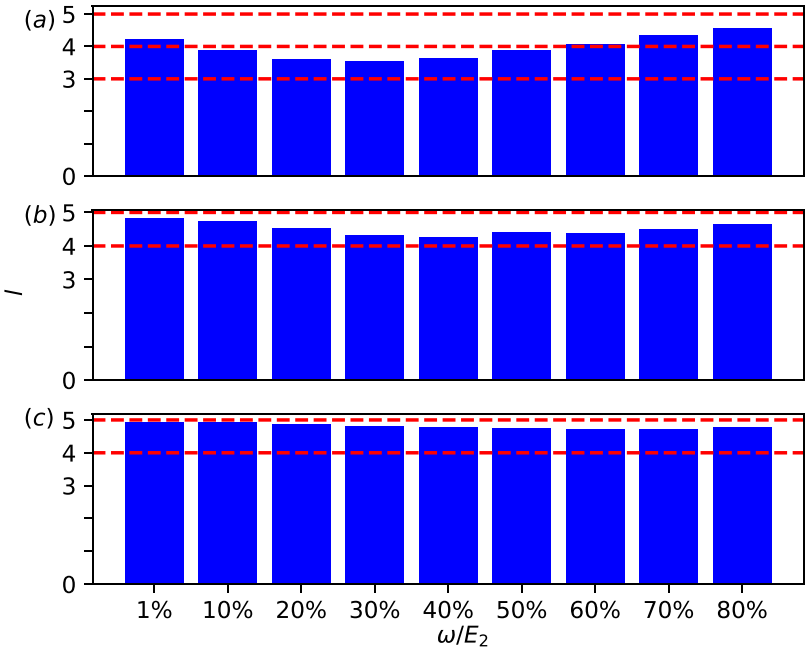

Figure 5. Photon energy—l distribution. The incident electron energy is (a) $E_2 = 5$ MeV, (b) $E_2 = 10$ MeV, (c) $E_2 = 20$ MeV. Abscissa values are different energy of outgoing photons which is shown as the ratio of photon energy to incident electron energy. Ordinate values are the outgoing photon average OAM projection.

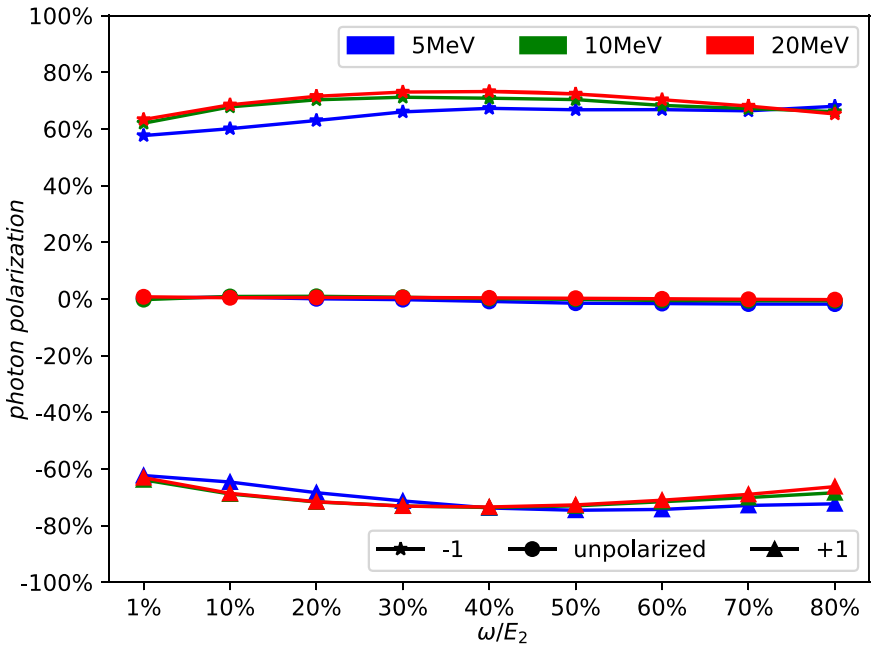

Figure 6. Photon polarization—photon energy distribution. Circle marker represents unpolarized incident electrons, triangle and star markers represent 100% polarized incident electrons with opposite polarization—+1 and −1, respectively. Three color curves respent $E_2 = 5$ MeV, $E_2 = 10$ MeV and $E_2 = 20$ MeV, respectively.

smaller in figure 5(b) ($E_2 = 10$ MeV), and the trend is slower in figure 5(c) ($E_2 = 20$ MeV). It indicates that the increase of energy will cause more OAM carried by the incident vortex electron transferred to outgoing vortex photon.

4.3. Polarization in triple-vortex bremsstrahlung

We calculate the polarization of outgoing photons in two cases: the incident electron is unpolarized and 100% polarized, as shown in figure 6. Circle marker shows that for the unpolarized incident electron, the photons polarization is less than 2%, that is, the outgoing photons are also unpolarized. Triangle and star

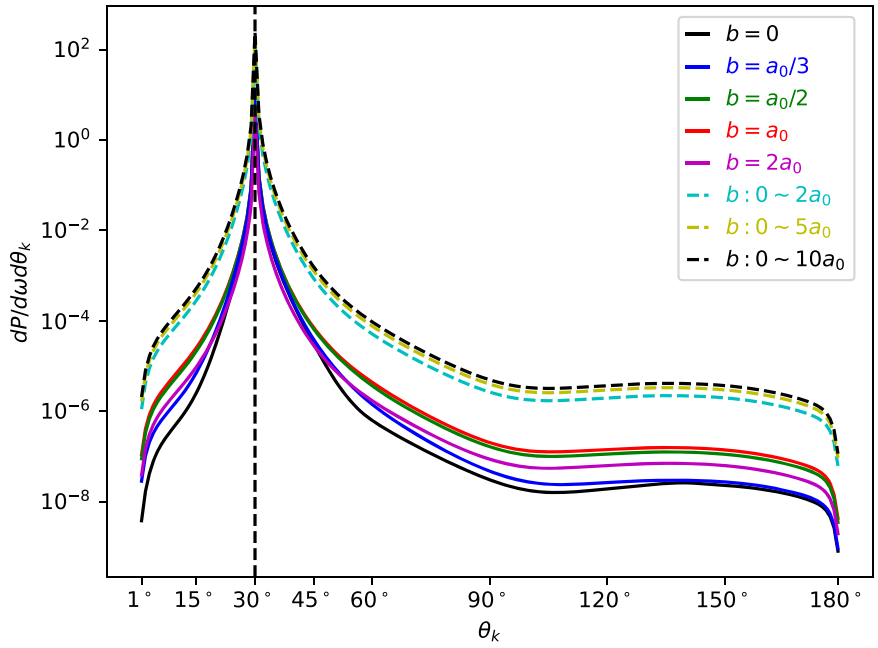

Figure 7. The opening angle of photon—probability distribution with different impact parameter b, with $E_2 = 5$ MeV, $\omega = 1$ MeV, $\theta_2 = 30°$, $m_2 = 5$, l from $-7- + 17$, n from $-10- + 10$. Solid curves with different colors represent $b = 0$, $b = a_0/3$, $b = a_0/2$, $b = a_0$ and $b = 2a_0$, respectively. The cyan, yellow and black dashed curves represent the integral range of $0–2a_0$, $0–5a_0$ and $0–10a_0$, respectively.

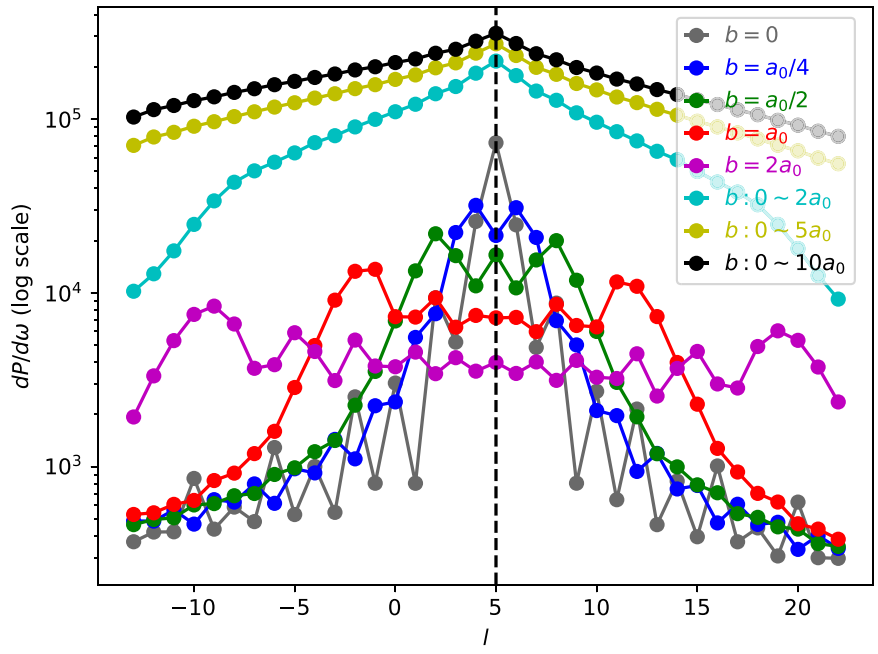

Figure 8. The l-probability distribution with different impact parameter b. $E_2 = 20$ MeV, $\omega = 1$ MeV, $m_2 = 5$, l ranges from $-22- + 22$, n ranges from $-20- + 20$. Each point represents the specified l value. Different colors represent different value of b marked in figure. The cyan, yellow and black points represent the integral range of b, which are $0–2a_0$, $0–5a_0$ and $0–10a_0$, respectively.

markers show 100% polarization of incident electrons with opposite polarization direction, the polarization of photons is much higher than that of unpolarized case. When the energy of outgoing photons increases from 1% to 50% of the energy of incident electrons, the polarization increases from 60% to 75%. When the

energy of photons continues to increase, the polarization begins to decay. Polarization of triple vortex bremsstrahlung is independent of the energy of incident electrons.

4.4. Influence of a non-zero impact parameter (*b*-dependence) in triple-vortex bremsstrahlung

The above analysis considers zero impact parameter between the incident electron wave packet and the nucleus electric field ($b = 0$). In the following we extend the discussion to the regime where the collision is not perfectly aligned, following the b-dependent differential scattering probability: equations (19) and (20). Figure 7 shows the b-dependent opening angle—probability distribution, where a_0 is the Bohr radius of corresponding nucleus. Different impact parameter b do not change the photon opening angle θ_k of maximum probability position which is equal to the opening angle θ_2 of incident electron. Although the profile of the distribution do not change significantly with b, the probability varies for θ_k away from the maximum position. We see that the scattering probability in these regions increases with larger impact parameter up to $b = a_0$ and then declines for $b = 2a_0$. In other words, highest probability is obtained when b equals the Bohr radius. The distributions integrated over b are also depicted in figure 7. Comparing the case of $0–5a_0$ and $0–10a_0$, we see that the probability already converges in these cases.

The l-probability distribution with different impact parameter is given in figure 8. Comparing the six profiles, it is found that when b increases gradually, the l distribution diffuses from $l = 5$ (equal to m_2 value carried by incident electrons) to both sides. The probability at the center decreases, while the one away from $l = 5$ grows. Multiple peaks are seen on both sides, while the average value remains constant. These lead to smooth of the l spectrum after integrating over a certain range of impact distance. The results indicate that the distribution detected in possible experiment would conform to the black and cyan points when considering a macroscopic target-an umbrella-like profile, taking $l = m_2$ as the highest point and descending slowly to both sides.

5. Conclusion

In the framework of QED, we calculate the triple-vortex bremsstrahlung which emitted electron, photon and incident electron are all vortex states in detail and obtain the scattering probability in the case of wave-packet described incident electron. The four Kronecker symbols emerging in matrix equation (7) indicate that TAM in this process is conserved. Through the numerical analysis of the scattering probability, we combine the two kinds of opening angle distribution to obtain the scattering characteristics that the opening angles of the outgoing vortex photon, electron and the incident vortex electron approach the same. This property provides us with a way to get the fixed opening angle vortex photons. We only need to control the opening angle of the incident vortex electrons to get the same outgoing vortex photon as the opening angle of the incident vortex electron. The OAM transfer of the triple-vortex bremsstrahlung is researched. The OAM of the incident vortex electron is more likely transferred to the outgoing photon rather than electron. And the spin-flip discrete symmetry of triple-vortex bremsstrahlung at high energy level is obtained by analyzing the influence of spin on the OAM-probability distribution. For other scattering processes in vortex states, the scattering cross section angular momentum distribution may have similar spin-flip discrete symmetry. Polarization is analyzed, which provides us with a method to generate high-energy polarized vortex photons through triple-vortex bremsstrahlung of highly polarized vortex electrons. Finally, non-zero impact parameter b is taken into account. The profile of the opening angle distribution for photons is not changed significantly with finite b while the l spectrum is notably modified. These properties are more in line with possible observations in real experiments.

Acknowledgments

This work is supported by the National Science Foundation of China (Nos. 11875307 and 11935008), the Strategic Priority Research Program of Chinese Academy of Sciences (Grant No. XDB16010000) and the Ministry of Science and Technology of the People's Republic of China (Grant No. 2018YFA0404803).

Data availability statement

The data that support the findings of this study are available upon reasonable request from the authors.

Appendix A. Orthogonality and normalization of the vortex states

Vortex photon:

$$\begin{aligned}(A^{j,\lambda;\mu}_{k_\perp,k_z}, A^{j',\lambda'}_{k'_\perp,k'_z;\mu}) &= \mathrm{i}\int \mathrm{d}^3x (A^{j,\lambda;\mu*}_{k_\perp,k_z}(x)\partial_t A^{j',\lambda'}_{k'_\perp,k'_z;\mu}(x) - \partial_t A^{j,\lambda;\mu*}_{k_\perp,k_z}(x) A^{j',\lambda'}_{k'_\perp,k'_z;\mu}(x))\\ &= \int \mathrm{d}^3x(\omega'+\omega) A^{j,\lambda;\mu*}_{k_\perp,k_z}(x) A^{j',\lambda'}_{k'_\perp,k'_z;\mu}(x)\\ &= \frac{1}{2k_\perp}\delta(k_\perp - k'_\perp)\delta(k_z-k'_z)\left[-\left(1+\frac{k_z^2}{\omega^2}\right)\delta_{\lambda,\lambda'}\delta_{j,j'} - (\delta_{\lambda,-\lambda'}+\lambda\lambda')\frac{k_\perp^2}{\omega^2}\delta_{j,j'}\right]\\ &= -\delta_{\lambda,\lambda'}\delta_{j,j'}\frac{1}{k_\perp}\delta(k_\perp-k'_\perp)\delta(k_z-k'_z). \end{aligned} \tag{A.1}$$

Vortex electron:

$$\begin{aligned}\int \mathrm{d}z\,\mathrm{d}\theta\,\mathrm{d}r\, r\psi^{\dagger s,m}_{p_\perp,p_z}(x)\psi^{s',m'}_{p'_\perp,p'_z}(x) &= \frac{1}{2}\delta_{m,m'}\frac{1}{p_\perp}\delta(p_\perp-p'_\perp)\delta(p_z-p'_z)\\ &\quad\times\left[\left(1+\frac{M}{E}\right)+\frac{p_z^2}{|\vec{p}|^2}\left(1-\frac{M}{E}\right)+\frac{p_\perp^2}{|\vec{p}|^2}\left(1-\frac{M}{E}\right)\right]\xi^{s\dagger}\xi^{s'}\\ &= \delta_{s,s'}\delta_{m,m'}\frac{1}{p_\perp}\delta(p_\perp-p'_\perp)\delta(p_z-p'_z). \end{aligned} \tag{A.2}$$

Vortex electron with impact parameter:

$$\begin{aligned}\int \mathrm{d}z\,\mathrm{d}\theta\,\mathrm{d}r\, r\psi^{\dagger s,m}_{p_\perp,p_z}(x,\vec{b})\psi^{s',m'}_{p'_\perp,p'_z}(x,\vec{b}) &= \frac{1}{2p_\perp}\delta(p_\perp-p'_\perp)\delta(p_z-p'_z)\sum_{n,n'}\mathrm{e}^{\mathrm{i}(n-n')\theta_b}J_n(p_\perp b)J_{n'}(p_\perp b)\delta_{m+n,m'+n'}\cdot\\ &\quad\times\left(\left(1+\frac{M}{E}\right)+\frac{p_z^2}{|\vec{p}|^2}\left(1-\frac{M}{E}\right)+\frac{p_\perp^2}{|\vec{p}|^2}\left(1-\frac{M}{E}\right)\right)\xi^{s\dagger}\xi^{s'}\\ &= \delta_{s,s'}\delta_{m,m'}\frac{1}{p_\perp}\delta(p_\perp-p'_\perp)\delta(p_z-p'_z). \end{aligned} \tag{A.3}$$

Appendix B. Derivation of *S*-matrix and coefficients of matrix elements

We define an operator given by the integral of the triple-Bessel product:

$$\begin{aligned}S_n^m(p,k,q) &= \int \mathrm{d}r\, rJ_n(pr)J_{m-n}(qr)J_m(kr)\\ &= \frac{(-1)^m}{2\pi Aera_{p,q,k}}\cos(n(\pi-\angle(p,q))+m(\pi-\angle(k,q)))\\ &= \frac{1}{2\pi Aera_{p,q,k}}\cos(n\angle(p,k)-(m-n)\angle(k,q)), \end{aligned} \tag{B.1}$$

where $Aera_{p,q,k}$ represents the area of the triangle formed by p, q, k.

S-matrix:

$$S_{fi} = S_1 + S_2 = -\mathrm{ie}^2\int \mathrm{d}^4x\,\mathrm{d}^4y\bar{\psi}_f(x)[\gamma^\mu A^*_\mu(x)S_F(x-y)\gamma^0A_0(y)+\gamma^0A_0(x)S_F(x-y)\gamma^\nu A^*_\nu(y)]\psi_i(y), \tag{B.2}$$

where

$$\gamma^\mu A^*_\mu(x) = \gamma^\mu(\epsilon_\mu \mathrm{e}^{\mathrm{i}k_z z-\mathrm{i}\omega t})^* = \gamma^\mu\epsilon^*_\mu\,\mathrm{e}^{-\mathrm{i}k_z z+\mathrm{i}\omega t}, \tag{B.3}$$

$$\gamma^\mu\epsilon^*_\mu = -\frac{1}{\sqrt{2}(2\pi)}\frac{1}{\sqrt{2\omega}}\begin{bmatrix}0 & \Lambda^{j,\lambda}_{k_\perp,k_z}(r,\theta)\\ -\Lambda^{j,\lambda}_{k_\perp,k_z}(r,\theta) & 0\end{bmatrix}, \tag{B.4}$$

$$\Lambda^{j,\lambda}_{k_\perp,k_z}(r,\theta)=\begin{bmatrix}\dfrac{\lambda k_\perp}{\omega}J_j(k_\perp r)\mathrm{e}^{-\mathrm{i}j\theta} & -\mathrm{i}\left(1-\dfrac{\lambda k_z}{\omega}\right)J_{j+1}(k_\perp r)\mathrm{e}^{-\mathrm{i}(j+1)\theta}\\ -\mathrm{i}\left(1+\dfrac{\lambda k_z}{\omega}\right)J_{j-1}(k_\perp r)\mathrm{e}^{-\mathrm{i}(j-1)\theta} & -\dfrac{\lambda k_\perp}{\omega}J_j(k_\perp r)\mathrm{e}^{-\mathrm{i}j\theta}\end{bmatrix}. \tag{B.5}$$

We first calculate S_1 in cylindrical coordinates:

$$\begin{aligned}S_1=&\frac{-\mathrm{i}Z\mathrm{e}^3}{32\pi^3\sqrt{\omega}}\int \mathrm{d}t\,\mathrm{d}z\,d\theta\,\mathrm{d}r\,r\mathrm{d}t'\,\mathrm{d}z'\,\mathrm{d}\theta'\,\mathrm{d}r'r'\,\mathrm{e}^{-\mathrm{i}p_{1z}z+\mathrm{i}E_1t}\cdot\\
&\times\left[\left(\sqrt{1+\frac{M}{E_1}}\xi^{s_1\dagger},-\sqrt{1-\frac{M}{E_1}}\frac{p_{1z}}{|\vec{p_1}|}\xi^{s_1\dagger}\sigma^3\right)J_{m_1}(p_{1\perp}r)\mathrm{e}^{-\mathrm{i}m_1\theta}-\frac{\mathrm{i}p_{1\perp}}{|\vec{p_1}|}\sqrt{1-\frac{M}{E_1}}(0,-\xi^{s_1\dagger}\sigma^{\perp\dagger})\right]\cdot\\
&\times\left[\begin{bmatrix}0 & \Lambda(r,\theta)\\ -\Lambda & 0\end{bmatrix}\mathrm{e}^{-\mathrm{i}k_zz+i\omega t}\int\frac{\mathrm{d}^4p}{(2\pi)^4}\frac{\mathrm{e}^{-\mathrm{i}p(x-y)}}{\not p-M+i\epsilon}\gamma^0\int\frac{\mathrm{d}^3q}{(2\pi)^3}\frac{\mathrm{e}^{\mathrm{i}\vec{q}\cdot\vec{y}}}{|\vec{q}|^2}\right]\cdot\\
&\times\left[\begin{bmatrix}\sqrt{1+\dfrac{M}{E_2}}\xi^{s_2}\\ \sqrt{1-\dfrac{M}{E_2}}\left(\dfrac{p_{2z}}{|\vec{p_2}|}\sigma^3\right)\xi^{s_2}\end{bmatrix}J_{m_2}(p_{2\perp}r')\mathrm{e}^{\mathrm{i}m_2\theta'}+\frac{\mathrm{i}p_{2\perp}}{|\vec{p_2}|}\sqrt{1-\frac{M}{E_2}}\begin{bmatrix}0\\ \sigma^\perp\xi^{s_2}\end{bmatrix}\right]\mathrm{e}^{\mathrm{i}p_{2z}z'-\mathrm{i}E_2t'}.\end{aligned} \tag{B.6}$$

The $\mathrm{e}^{-\mathrm{i}qy}$ and $\mathrm{e}^{-\mathrm{i}p(x-y)}$ in the cylindrical coordinates can be expanded into:

$$\mathrm{e}^{-\mathrm{i}qy}=\mathrm{e}^{\mathrm{i}q_zz'-\mathrm{i}q^0t'}\sum_{n_3}\mathrm{i}^{n_3}J_{n_3}(q_\perp r')\mathrm{e}^{\mathrm{i}n_3\theta'-\mathrm{i}n_3\phi_q}, \tag{B.7}$$

$$\mathrm{e}^{-\mathrm{i}p(x-y)}=\mathrm{e}^{\mathrm{i}p_zz-\mathrm{i}E_pt}\sum_{n_1}\mathrm{i}^{n_1}J_{n_1}(p_\perp r)\mathrm{e}^{\mathrm{i}n_1\theta-\mathrm{i}n_1\phi_p}\cdot\mathrm{e}^{-\mathrm{i}p_zz'+\mathrm{i}E_pt'}\sum_{n_2}\mathrm{i}^{-n_2}J_{n_2}(p_\perp r')\mathrm{e}^{-\mathrm{i}n_2\theta'+\mathrm{i}n_2\phi_p}, \tag{B.8}$$

$$\cos\,\phi_q=\frac{q^1}{q_\perp}, \tag{B.9}$$

$$\cos\,\phi_p=\frac{p^1}{p_\perp}. \tag{B.10}$$

Then, we have:

$$\begin{aligned}S_1=&\frac{-\mathrm{i}Z\mathrm{e}^3}{32\pi^3\sqrt{\omega}}\int\mathrm{d}t\,\mathrm{d}z\,\mathrm{d}\theta\,\mathrm{d}r\,r\mathrm{d}t'\,\mathrm{d}z'\,\mathrm{d}\theta'\,\mathrm{d}r'\,r'\cdot\\
&\times\mathrm{e}^{\mathrm{i}(-p_{1z}-k_z+p_z)z}\mathrm{e}^{\mathrm{i}(E_1+\omega-E_p)t}\mathrm{e}^{\mathrm{i}(-p_z+q_z+p_{2z})z'}\mathrm{e}^{\mathrm{i}(E_p-q^0-E_2)t'}\cdot\\
&\times\sum_{n_1}\mathrm{i}^{n_1}J_{n_1}(p_\perp r)\mathrm{e}^{\mathrm{i}n_1\theta-\mathrm{i}n_1\phi_p}\sum_{n_2}\mathrm{i}^{-n_2}J_{n_2}(p_\perp r')\mathrm{e}^{-\mathrm{i}n_2\theta'+\mathrm{i}n_2\phi_p}\sum_{n_3}\mathrm{i}^{n_3}J_{n_3}(q_\perp r')\mathrm{e}^{\mathrm{i}n_3\theta'-\mathrm{i}n_3\phi_q}\cdot\\
&\times\left[\left(\sqrt{1+\frac{M}{E_1}}\xi^{s_1\dagger},-\sqrt{1-\frac{M}{E_1}}\frac{p_{1z}}{|\vec{p_1}|}\xi^{s_1\dagger}\sigma^3\right)J_{m_1}(p_{1\perp}r)\mathrm{e}^{-\mathrm{i}m_1\theta}-\frac{\mathrm{i}p_{1\perp}}{|\vec{p_1}|}\sqrt{1-\frac{M}{E_1}}(0,-\xi^{s_1\dagger}\sigma^{\perp\dagger})\right]\cdot\\
&\times\left[\begin{bmatrix}0 & \Lambda(r,\theta)\\ -\Lambda & 0\end{bmatrix}\int\frac{\mathrm{d}^4p}{(2\pi)^4}\frac{1}{\not p-M+\mathrm{i}\epsilon}\gamma^0\int\frac{\mathrm{d}^4q}{(2\pi)^3}\frac{1}{|\vec{q}|^2}\delta(q^0)\right]\cdot\\
&\times\left[\begin{bmatrix}\sqrt{1+\dfrac{M}{E_2}}\xi^{s_2}\\ \sqrt{1-\dfrac{M}{E_2}}\left(\dfrac{p_{2z}}{|\vec{p_2}|}\sigma^3\right)\xi^{s_2}\end{bmatrix}J_{m_2}(p_{2\perp}r')\mathrm{e}^{\mathrm{i}m_2\theta'}+\frac{\mathrm{i}p_{2\perp}}{|\vec{p_2}|}\sqrt{1-\frac{M}{E_2}}\begin{bmatrix}0\\ \sigma^\perp\xi^{s_2}\end{bmatrix}\right]\\
=&\frac{-\mathrm{i}Z\mathrm{e}^3}{32\pi^3\sqrt{\omega}}\int\mathrm{d}\theta\,\mathrm{d}r\,r\mathrm{d}\theta'\,\mathrm{d}r'\,r'\int\frac{\mathrm{d}^4p\,\mathrm{d}^4q}{(2\pi)^3}\cdot\delta(q^0)\delta(-p_{1z}-k_z+p_z)\delta(E_1+\omega-E_p)\delta(-p_z+q_z+p_{2z})\\
&\times\delta(E_p-q^0-E2)\cdot\sum_{n_1,n_2,n_3}\mathrm{i}^{n_1-n_2+n_3}J_{n_1}(p_\perp r)J_{n_2}(p_\perp r')J_{n_3}(q_\perp r')\mathrm{e}^{\mathrm{i}n_1\theta-\mathrm{i}n_2\theta'+\mathrm{i}n_3\theta'}\\
&\times\mathrm{e}^{-\mathrm{i}n_1\phi_p+\mathrm{i}n_2\phi_p-\mathrm{i}n_3\phi_q}\cdot\left[\left(\sqrt{1+\frac{M}{E_1}}\xi^{s_1\dagger},-\sqrt{1-\frac{M}{E_1}}\frac{p_{1z}}{|\vec{p_1}|}\xi^{s_1\dagger}\sigma^3\right)J_{m_1}(p_{1\perp}r)\mathrm{e}^{-\mathrm{i}m_1\theta}\right.\\
&\left.-\frac{\mathrm{i}p_{1\perp}}{|\vec{p_1}|}\sqrt{1-\frac{M}{E_1}}(0,-\xi^{s_1\dagger}\sigma^{\perp\dagger})\right]\cdot\left[\begin{bmatrix}0 & \Lambda(r,\theta)\\ -\Lambda & 0\end{bmatrix}\frac{1}{\not p-M+\mathrm{i}\epsilon}\gamma^0\frac{1}{|\vec{q}|^2}\right]\cdot\end{aligned}$$

$$\times \left[\begin{bmatrix} \sqrt{1+\frac{M}{E_2}}\xi^{s_2} \\ \sqrt{1-\frac{M}{E_2}}\left(\frac{p_{2z}}{|\vec{p_2}|}\sigma^3\right)\xi^{s_2}\end{bmatrix} J_{m_2}(p_{2\perp}r')\mathrm{e}^{\mathrm{i}m_2\theta'} + \frac{\mathrm{i}p_{2\perp}}{|\vec{p_2}|}\sqrt{1-\frac{M}{E_2}}\begin{bmatrix}0\\ \sigma^{\perp}\xi^{s_2}\end{bmatrix}\right]. \tag{B.11}$$

In the cylindrical coordinates:

$$\mathrm{d}^4p\,\mathrm{d}^4q = \mathrm{d}E_p\,\mathrm{d}p_z\,\mathrm{d}\phi_p\,\mathrm{d}p_\perp p_\perp\,\mathrm{d}q^0\,\mathrm{d}q_z\,\mathrm{d}\phi_q\,\mathrm{d}q_\perp\,q_\perp. \tag{B.12}$$

Use δ functions to integrate:

$$\begin{aligned} S_1 = {} & \frac{-\mathrm{i}Z\mathrm{e}^3}{32\pi^3\sqrt{\omega}}\int \mathrm{d}\theta\,\mathrm{d}r\,r\mathrm{d}\theta'\,\mathrm{d}r'\,r'\frac{\mathrm{d}\phi_p\mathrm{d}p_\perp p_\perp\mathrm{d}\phi_q\mathrm{d}q_\perp q_\perp}{(2\pi)^3}\delta(E_1+\omega-E_2)\cdot \\ & \times\sum_{n_1,n_2,n_3}\mathrm{i}^{n_1-n_2+n_3}J_{n_1}(p_\perp r)J_{n_2}(p_\perp r')J_{n_3}(q_\perp r')\mathrm{e}^{\mathrm{i}n_1\theta-\mathrm{i}n_2\theta'+\mathrm{i}n_3\theta'}\mathrm{e}^{-\mathrm{i}n_1\phi_p+\mathrm{i}n_2\phi_p-\mathrm{i}n_3\phi_q}. \\ & \times\left[\left(\sqrt{1+\frac{M}{E_1}}\xi^{s_1\dagger},-\sqrt{1-\frac{M}{E_1}}\frac{p_{1z}}{|\vec{p_1}|}\xi^{s_1\dagger}\sigma^3\right)J_{m_1}(p_{1\perp}r)\mathrm{e}^{-\mathrm{i}m_1\theta}-\frac{\mathrm{i}p_{1\perp}}{|\vec{p_1}|}\sqrt{1-\frac{M}{E_1}}(0,-\xi^{s_1\dagger}\sigma^{\perp\dagger})\right]\cdot \\ & \times\left[\begin{bmatrix}0 & \Lambda(r,\theta)\\ -\Lambda & 0\end{bmatrix}\frac{1}{\not{p}-M+\mathrm{i}\epsilon}\gamma^0\frac{1}{|\vec{q}|^2}\right]\cdot\left[\begin{bmatrix}\sqrt{1+\frac{M}{E_2}}\xi^{s_2}\\ \sqrt{1-\frac{M}{E_2}}\left(\frac{p_{2z}}{|\vec{p_2}|}\sigma^3\right)\xi^{s_2}\end{bmatrix}J_{m_2}(p_{2\perp}r')e^{im_2\theta'}\right. \\ & \left.+\frac{\mathrm{i}p_{2\perp}}{|\vec{p_2}|}\sqrt{1-\frac{M}{E_2}}\begin{bmatrix}0\\ \sigma^{\perp}\xi^{s_2}\end{bmatrix}\right]|_{q^0=0,p_z=p_{1z}+k_z,q_z=p_{1z}+k_z-p_{2z},E_p=E_2}. \end{aligned} \tag{B.13}$$

Integrating over ϕ_q, n_3:

$$\begin{aligned} S_1 = {} & \frac{-\mathrm{i}Z\mathrm{e}^3}{32\pi^3}\int \mathrm{d}\theta\,\mathrm{d}r\,r\mathrm{d}\theta'\,\mathrm{d}r'r'\frac{\mathrm{d}\phi_p\mathrm{d}p_\perp\,p_\perp\,\mathrm{d}q_\perp\,q_\perp}{(2\pi)^2}\delta(E_1+\omega-E_2)\cdot\frac{\sqrt{(E_1-M)(E_2-M)}}{\sqrt{\omega E_1E_2}}\cdot \\ & \times\frac{1}{(p^2-M^2)\cdot|\vec{p_1}|\cdot|\vec{p_2}|\cdot|\vec{q}|^2}\cdot\sum_{n_1,n_2}\mathrm{i}^{n_1-n_2}J_{n_1}(p_\perp r)J_{n_2}(p_\perp r')J_0(q_\perp r')\mathrm{e}^{\mathrm{i}n_1\theta-\mathrm{i}n_2\theta'}\mathrm{e}^{-\mathrm{i}n_1\phi_p+\mathrm{i}n_2\phi_p}. \\ & \times\left[((E_1+M)\xi^{s_1\dagger},-p_{1z}\xi^{s_1\dagger}\sigma^3)J_{m_1}(p_{1\perp}r)\mathrm{e}^{-\mathrm{i}m_1\theta}-\mathrm{i}p_{1\perp}(0,-\xi^{s_1\dagger}\sigma^{\perp\dagger})\right]\cdot \\ & \times\left[\begin{bmatrix}0 & \Lambda(r,\theta)\\ -\Lambda & 0\end{bmatrix}(\not{p}+M)\gamma^0\right]\cdot\left[\begin{bmatrix}(E_2+M)\xi^{s_2}\\ (p_{2z}\sigma^3)\xi^{s_2}\end{bmatrix}J_{m_2}(p_{2\perp}r')\mathrm{e}^{\mathrm{i}m_2\theta'}+\mathrm{i}p_{2\perp}\begin{bmatrix}0\\ \sigma^{\perp}\xi^{s_2}\end{bmatrix}\right] \\ & \times|_{q^0=0,p_z=p_{1z}+k_z,q_z=p_{1z}+k_z-p_{2z},E_p=E_2,n_3=0}, \end{aligned} \tag{B.14}$$

where

$$\not{p}+M = \begin{bmatrix}E_p+M & -\vec{\sigma}\cdot\vec{p}\\ \vec{\sigma}\cdot\vec{p} & -(E_p-M)\end{bmatrix}, \tag{B.15}$$

$$(\not{p}+M)\gamma^0 = \begin{bmatrix}E_p+M & \vec{\sigma}\cdot\vec{p}\\ \vec{\sigma}\cdot\vec{p} & E_p-M\end{bmatrix}, \tag{B.16}$$

$$\vec{\sigma}\cdot\vec{p} = \begin{bmatrix}p^3 & p^1-\mathrm{i}p^2\\ p^1+\mathrm{i}p^2 & -p^3\end{bmatrix} = \begin{bmatrix}p_z & p_\perp\mathrm{e}^{-\mathrm{i}\phi_p}\\ p_\perp\mathrm{e}^{\mathrm{i}\phi_p} & -p_z\end{bmatrix}. \tag{B.17}$$

The integral of ϕ_p:

$$\begin{aligned} \mathrm{i}^{n_1-n_2}\int\mathrm{d}\phi_p\,\mathrm{e}^{\mathrm{i}(-n_1+n_2)\phi_p}\vec{\sigma}\cdot\vec{p} &= \mathrm{i}^{n_1-n_2}\int\mathrm{d}\phi_p\,\mathrm{e}^{\mathrm{i}(-n_1+n_2)\phi_p}\begin{bmatrix}p^3 & p^1-\mathrm{i}p^2\\ p^1+\mathrm{i}p^2 & -p^3\end{bmatrix} \\ &= \mathrm{i}^{n_1-n_2}\int\mathrm{d}\phi_p\,\mathrm{e}^{\mathrm{i}(-n_1+n_2)\phi_p}\begin{bmatrix}p_z & p_\perp\mathrm{e}^{-\mathrm{i}\phi_p}\\ p_\perp\mathrm{e}^{\mathrm{i}\phi_p} & -p_z\end{bmatrix} \\ &= 2\pi\cdot\begin{bmatrix}p_z\delta(n_1-n_2) & -\mathrm{i}p_\perp\delta(n_1-n_2+1)\\ \mathrm{i}p_\perp\delta(n_1-n_2-1) & -p_z\delta(n_1-n_2)\end{bmatrix}. \end{aligned} \tag{B.18}$$

We define

$$Q^{n_1,n_2}_{p_z,p_\perp} = \begin{bmatrix} p_z\delta(n_1-n_2) & -\mathrm{i}p_\perp\delta(n_1-n_2+1) \\ \mathrm{i}p_\perp\delta(n_1-n_2-1) & -p_z\delta(n_1-n_2) \end{bmatrix}, \tag{B.19}$$

$$\mathrm{i}^{n_1-n_2}\int \mathrm{d}\phi_p\, \mathrm{e}^{\mathrm{i}(-n_1+n_2)\phi_p}\vec{\sigma}\cdot\vec{p} = 2\pi Q^{n_1,n_2}_{p_z,p_\perp}. \tag{B.20}$$

So:

$$\mathrm{i}^{n_1-n_2}\int \mathrm{d}\phi_p\, \mathrm{e}^{\mathrm{i}(-n_1+n_2)\phi_p}(\not{p}+M)\gamma^0 = 2\pi\cdot\begin{bmatrix} (E_p+M)\delta(n_1-n_2) & Q^{n_1,n_2}_{p_z,p_\perp} \\ Q^{n_1,n_2}_{p_z,p_\perp} & (E_p-M)\delta(n_1-n_2) \end{bmatrix}. \tag{B.21}$$

$$\begin{aligned} S_1 = {} & \frac{-\mathrm{i}Z\mathrm{e}^3}{32\pi^3}\int \mathrm{d}\theta\,\mathrm{d}r\,r\mathrm{d}\theta'\,\mathrm{d}r'\,r'\frac{\mathrm{d}p_\perp p_\perp\,\mathrm{d}q_\perp q_\perp}{(2\pi)}\delta(E_1+\omega-E_2)\cdot\frac{\sqrt{(E_1-M)(E_2-M)}}{\sqrt{\omega E_1 E_2}}\cdot \\ & \times\frac{1}{(p^2-M^2)\cdot|\vec{p}_1|\cdot|\vec{p}_2|\cdot|\vec{q}|^2}\cdot\sum_{n_1,n_2}J_{n_1}(p_\perp r)J_{n_2}(p_\perp r')J_0(q_\perp r')\mathrm{e}^{\mathrm{i}n_1\theta-\mathrm{i}n_2\theta'}\cdot \\ & \times\left[((E_1+M)\xi^{s_1\dagger},-p_{1z}\xi^{s_1\dagger}\sigma^3)J_{m_1}(p_{1\perp}r)\mathrm{e}^{-\mathrm{i}m_1\theta}-\mathrm{i}p_{1\perp}(0,-\xi^{s_1\dagger}\sigma^{\perp\dagger})\right]\cdot\begin{bmatrix} 0 & \Lambda(r,\theta) \\ -\Lambda & 0 \end{bmatrix}\cdot \\ & \times\begin{bmatrix} (E_p+M)\delta(n_1-n_2) & Q^{n_1,n_2}_{p_z,p_\perp} \\ Q^{n_1,n_2}_{p_z,p_\perp} & (E_p-M)\delta(n_1-n_2) \end{bmatrix}\cdot\left[\begin{bmatrix} (E_2+M)\xi^{s_2} \\ (p_{2z}\sigma^3)\xi^{s_2} \end{bmatrix}J_{m_2}(p_{2\perp}r')e^{im_2\theta'}+ip_{2\perp}\begin{bmatrix} 0 \\ \sigma^\perp\xi^{s_2} \end{bmatrix}\right] \\ & \times|_{q^0=0,p_z=p_{1z}+k_z,q_z=p_{1z}+k_z-p_{2z},E_p=E_2,n_3=0} \end{aligned} \tag{B.22}$$

$$\begin{aligned} & \sum_{n_1,n_2}J_{n_1}(p_\perp r)J_{n_2}(p_\perp r')J_0(q_\perp r')\mathrm{e}^{\mathrm{i}n_1\theta-\mathrm{i}n_2\theta'}\cdot\begin{bmatrix} (E_p+M)\delta(n_1-n_2) & Q^{n_1,n_2}_{p_z,p_\perp} \\ Q^{n_1,n_2}_{p_z,p_\perp} & (E_p-M)\delta(n_1-n_2) \end{bmatrix} \\ & \quad=\sum_{n_1}J_{n_1}(p_\perp r)J_{n_2}(p_\perp r')J_0(q_\perp r')\mathrm{e}^{\mathrm{i}n_1\theta-\mathrm{i}n_2\theta'}\cdot\begin{bmatrix} (E_p+M)|_{n_2=n_1} & Q_{p_z,p_\perp} \\ Q_{p_z,p_\perp} & (E_p-M)|_{n_2=n_1} \end{bmatrix} \end{aligned} \tag{B.23}$$

$$Q_{p_z,p_\perp} = \begin{bmatrix} p_z|_{n_2=n_1} & -\mathrm{i}p_\perp|_{n_2=n_1+1} \\ \mathrm{i}p_\perp|_{n_2=n_1-1} & -p_z|_{n_2=n_1} \end{bmatrix} \tag{B.24}$$

$$\begin{aligned} S_1 = {} & \frac{-\mathrm{i}Z\mathrm{e}^3}{32\pi^3}\delta(E_1+\omega-E_2)\frac{\sqrt{(E_1-M)(E_2-M)}}{\sqrt{\omega E_1E_2}}\cdot\int\frac{\mathrm{d}q_\perp\,\mathrm{d}p_\perp}{2\pi}\cdot\frac{q_\perp p_\perp}{(p^2-M^2)\cdot|\vec{p}_1|\cdot|\vec{p}_2|\cdot|\vec{q}|^2}\cdot\xi^{s_1\dagger}\cdot \\ & \times\int\mathrm{d}\theta\,\mathrm{d}r\,r\mathrm{d}\theta'\,\mathrm{d}r'\,r'\sum_{n_1}J_{n_1}(p_\perp r)J_{n_2}(p_\perp r')J_0(q_\perp r')\mathrm{e}^{\mathrm{i}n_1\theta-\mathrm{i}n_2\theta'}\cdot \\ & \times\left[(E_1+M)J_{m_1}(p_{1\perp}r)\mathrm{e}^{-\mathrm{i}m_1\theta},-p_{1z}\sigma^3J_{m_1}(p_{1\perp}r)\mathrm{e}^{-\mathrm{i}m_1\theta}+\mathrm{i}p_{1\perp}\sigma^{\perp\dagger}\right]\cdot \\ & \times\begin{bmatrix} \Lambda(r,\theta)Q_{p_z,p_\perp} & \Lambda(r,\theta)(E_p-M)|_{n_2=n_1} \\ -\Lambda(r,\theta)(E_p+M)|_{n_2=n_1} & -\Lambda(r,\theta)Q_{p_z,p_\perp} \end{bmatrix}\cdot\begin{bmatrix} (E_2+M)J_{m_2}(p_{2\perp}r')\mathrm{e}^{\mathrm{i}m_2\theta'} \\ (p_{2z}\sigma^3)J_{m_2}(p_{2\perp}r')\mathrm{e}^{\mathrm{i}m_2\theta'}+\mathrm{i}p_{2\perp}\sigma^\perp \end{bmatrix}\cdot\xi^{s_2} \\ & \times|_{q^0=0,p_z=p_{1z}+k_z,q_z=p_{1z}+k_z-p_{2z},E_p=E_2,n_3=0} \end{aligned} \tag{B.25}$$

$$\sigma^\perp_{m_2,p_\perp}(r',\theta') = \begin{bmatrix} 0 & -J_{m_2-1}(p_\perp r')\mathrm{e}^{\mathrm{i}(m_2-1)\theta'} \\ J_{m_2+1}(p_\perp r')\mathrm{e}^{\mathrm{i}(m_2+1)\theta'} & 0 \end{bmatrix} \tag{B.26}$$

Put θ', r' into the last matrix and integrate:

$$\begin{aligned} & \int\mathrm{d}\theta'\,\mathrm{d}r'\,r'J_{n_2}(p_\perp r')J_0(q_\perp r')\mathrm{e}^{-\mathrm{i}n_2\theta'}\begin{bmatrix} (E_2+M)J_{m_2}(p_{2\perp}r')\mathrm{e}^{\mathrm{i}m_2\theta'} \\ (p_{2z}\sigma^3)J_{m_2}(p_{2\perp}r')\mathrm{e}^{\mathrm{i}m_2\theta'}+\mathrm{i}p_{2\perp}\sigma^\perp \end{bmatrix} \\ & \quad=2\pi\int\mathrm{d}r'\,r'J_{n_2}(p_\perp r')J_0(q_\perp r')\begin{bmatrix} (E_2+M)J_{m_2}(p_{2\perp}r')\delta(m_2-n_2) \\ (p_{2z}\sigma^3)J_{m_2}(p_{2\perp}r')\delta(m_2-n_2)+\mathrm{i}p_{2\perp}\sigma^{\perp'} \end{bmatrix} \\ & \quad=2\pi\begin{bmatrix} (E_2+M)S_0^{m_2}\delta(m_2-n_2) \\ (p_{2z}\sigma^3)S_0^{m_2}\delta(m_2-n_2)+\mathrm{i}p_{2\perp}\sigma^{\perp''} \end{bmatrix}, \end{aligned} \tag{B.27}$$

where

$$S_0^{m_2} = S_0^{m_2}(q_\perp, p_{2\perp}, p_\perp), \tag{B.28}$$

$$\sigma^{\perp'}_{m_2,p_\perp}(r',\theta') = \begin{bmatrix} 0 & -J_{m_2-1}(p_\perp r')\delta(m_2-1-n_2) \\ J_{m_2+1}(p_\perp r')\delta(m_2+1-n_2) & 0 \end{bmatrix}, \tag{B.29}$$

$$\sigma^{\perp''}_{m_2,p_\perp}(r',\theta') = \begin{bmatrix} 0 & -S_0^{m_2-1}\delta(m_2-1-n_2) \\ S_0^{m_2+1}\delta(m_2+1-n_2) & 0 \end{bmatrix}. \tag{B.30}$$

S_1 becomes:

$$\begin{aligned} S_1 = {} & \frac{-\mathrm{i}Ze^3}{32\pi^3}\delta(E_1+\omega-E_2)\frac{\sqrt{(E_1-M)(E_2-M)}}{\sqrt{\omega E_1 E_2}}\cdot\int \mathrm{d}q_\perp\,\mathrm{d}p_\perp\cdot\frac{q_\perp p_\perp}{(p^2-M^2)\cdot|\vec{p}_1|\cdot|\vec{p}_2|\cdot|\vec{q}|^2}\cdot\xi^{s_1\dagger}\cdot \\ & \times\int \mathrm{d}\theta\,\mathrm{d}r\,r\sum_{n_1}J_{n_1}(p_\perp r)\mathrm{e}^{\mathrm{i}n_1\theta}\cdot\left[(E_1+M)J_{m_1}(p_{1\perp}r)\mathrm{e}^{-\mathrm{i}m_1\theta},-p_{1z}\sigma^3J_{m_1}(p_{1\perp}r)\mathrm{e}^{-\mathrm{i}m_1\theta}+\mathrm{i}p_{1\perp}\sigma^{\perp\dagger}\right]\cdot \\ & \times\begin{bmatrix}\Lambda(r,\theta)Q_{p_z,p_\perp} & \Lambda(r,\theta)(E_p-M)|_{n_2=n_1}\\ -\Lambda(r,\theta)(E_p+M)|_{n_2=n_1} & -\Lambda(r,\theta)Q_{p_z,p_\perp}\end{bmatrix}\cdot\begin{bmatrix}(E_2+M)S_0^{m_2}\delta(m_2-n_2)\\ (p_{2z}\sigma^3)S_0^{m_2}\delta(m_2-n_2)+\mathrm{i}p_{2\perp}\sigma^{\perp''}\end{bmatrix}\cdot\xi^{s_2} \\ & \times|_{q^0=0,p_z=p_{1z}+k_z,q_z=p_{1z}+k_z-p_{2z},E_p=E_2,n_3=0}. \end{aligned} \tag{B.31}$$

We define:

$$\begin{aligned} \Xi_1 = {} & \int \mathrm{d}\theta\,\mathrm{d}r\,r\sum_{n_1}J_{n_1}(p_\perp r)\mathrm{e}^{\mathrm{i}n_1\theta}\cdot[(E_1+M)J_{m_1}(p_{1\perp}r)\mathrm{e}^{-\mathrm{i}m_1\theta},-p_{1z}\sigma^3J_{m_1}(p_{1\perp}r)\mathrm{e}^{-\mathrm{i}m_1\theta}+\mathrm{i}p_{1\perp}\sigma^{\perp\dagger}]\cdot \\ & \times\begin{bmatrix}\Lambda(r,\theta)Q_{p_z,p_\perp} & \Lambda(r,\theta)(E_p-M)|_{n_2=n_1}\\ -\Lambda(r,\theta)(E_p+M)|_{n_2=n_1} & -\Lambda(r,\theta)Q_{p_z,p_\perp}\end{bmatrix}\cdot\begin{bmatrix}(E_2+M)S_0^{m_2}\delta(m_2-n_2)\\ (p_{2z}\sigma^3)S_0^{m_2}\delta(m_2-n_2)+\mathrm{i}p_{2\perp}\sigma^{\perp''}\end{bmatrix} \\ & \times|_{q^0=0,p_z=p_{1z}+k_z,q_z=p_{1z}+k_z-p_{2z},E_p=E_2,n_3=0} \\ = {} & \int \mathrm{d}\theta\,\mathrm{d}r\,r\sum_{n_1}J_{n_1}(p_\perp r)\mathrm{e}^{\mathrm{i}n_1\theta}\cdot\Big[(E_1+M)J_{m_1}(p_{1\perp}r)\mathrm{e}^{-\mathrm{i}m_1\theta}\Lambda(r,\theta)Q_{p_z,p_\perp}+\big(p_{1z}\sigma^3J_{m_1}(p_{1\perp}r)\mathrm{e}^{-\mathrm{i}m_1\theta} \\ & -\mathrm{i}p_{1\perp}\sigma^{\perp\dagger}\big)\Lambda(r,\theta)(E_p+M)|_{n_2=n_1},(E_1+M)J_{m_1}(p_{1\perp}r)\mathrm{e}^{-\mathrm{i}m_1\theta}\Lambda(r,\theta)(E_p-M)|_{n_2=n_1} \\ & +(p_{1z}\sigma^3J_{m_1}(p_{1\perp}r)\mathrm{e}^{-\mathrm{i}m_1\theta}-\mathrm{i}p_{1\perp}\sigma^{\perp\dagger})\Lambda(r,\theta)Q_{p_z,p_\perp}\Big]\cdot\begin{bmatrix}(E_2+M)S_0^{m_2}\delta(m_2-n_2)\\ (p_{2z}\sigma^3)S_0^{m_2}\delta(m_2-n_2)+\mathrm{i}p_{2\perp}\sigma^{\perp''}\end{bmatrix} \\ & \times|_{q^0=0,p_z=p_{1z}+k_z,q_z=p_{1z}+k_z-p_{2z},E_p=E_2,n_3=0}. \end{aligned} \tag{B.32}$$

The integral of θ, r:

$$\begin{aligned} \Gamma_1 = {} & \int \mathrm{d}\theta\,\mathrm{d}r\,r\sum_{n_1}J_{n_1}(p_\perp r)\mathrm{e}^{\mathrm{i}n_1\theta}J_{m_1}(p_{1\perp}r)\mathrm{e}^{-\mathrm{i}m_1\theta}\Lambda(r,\theta) \\ = {} & \int \mathrm{d}\theta\,\mathrm{d}r\,r\sum_{n_1}J_{n_1}(p_\perp r)\mathrm{e}^{\mathrm{i}n_1\theta}J_{m_1}(p_{1\perp}r)\mathrm{e}^{-\mathrm{i}m_1\theta}\cdot \\ & \times\begin{bmatrix}\frac{\lambda k_\perp}{\omega}J_j(k_\perp r)\mathrm{e}^{-\mathrm{i}j\theta} & -\mathrm{i}\left(1-\frac{\lambda k_z}{\omega}\right)J_{j+1}(k_\perp r)\mathrm{e}^{-\mathrm{i}(j+1)\theta}\\ -\mathrm{i}\left(1+\frac{\lambda k_z}{\omega}\right)J_{j-1}(k_\perp r)\mathrm{e}^{-\mathrm{i}(j-1)\theta} & -\frac{\lambda k_\perp}{\omega}J_j(k_\perp r)\mathrm{e}^{-\mathrm{i}j\theta}\end{bmatrix} \\ = {} & \sum_{n_1}\begin{bmatrix}\frac{\lambda k_\perp}{\omega}S_j^{m_1+j}\delta(n_1-m_1-j) & -\mathrm{i}\left(1-\frac{\lambda k_z}{\omega}\right)S_{j+1}^{m_1+j+1}\delta(n_1-m_1-j-1)\\ -\mathrm{i}\left(1+\frac{\lambda k_z}{\omega}\right)S_{j-1}^{m_1+j-1}\delta(n_1-m_1-j+1) & -\frac{\lambda k_\perp}{\omega}S_j^{m_1+j}\delta(n_1-m_1-j)\end{bmatrix} \\ = {} & \begin{bmatrix}\frac{\lambda k_\perp}{\omega}S_j^{m_1+j}|_{n_1=m_1+j} & -\mathrm{i}\left(1-\frac{\lambda k_z}{\omega}\right)S_{j+1}^{m_1+j+1}|_{n_1=m_1+j+1}\\ -\mathrm{i}\left(1+\frac{\lambda k_z}{\omega}\right)S_{j-1}^{m_1+j-1}|_{n_1=m_1+j-1} & -\frac{\lambda k_\perp}{\omega}S_j^{m_1+j}|_{n_1=m_1+j}\end{bmatrix}, \end{aligned} \tag{B.33}$$

where

$$S_j^{m_1+j} = S_j^{m_1+j}(k_\perp, p_\perp, p_{1\perp}). \tag{B.34}$$

$$\begin{aligned}
\Gamma_2 &= \int \mathrm{d}\theta\, \mathrm{d}r\, r \sum_{n_1} J_{n_1}(p_\perp r)\mathrm{e}^{\mathrm{i}n_1\theta}\sigma^{\perp\dagger}\Lambda(r,\theta) \\
&= \int \mathrm{d}\theta\, \mathrm{d}r r \sum_{n_1} J_{n_1}(p_\perp r)\mathrm{e}^{\mathrm{i}n_1\theta}\begin{bmatrix} 0 & J_{m_1+1}(p_{1\perp}r)\mathrm{e}^{-\mathrm{i}(m_1+1)\theta} \\ -J_{m_1-1}(p_{1\perp}r)\mathrm{e}^{-\mathrm{i}(m_1-1)\theta} & 0 \end{bmatrix}\cdot \\
&\quad\times\begin{bmatrix} \dfrac{\lambda k_\perp}{\omega}J_j(k_\perp r)\mathrm{e}^{-\mathrm{i}j\theta} & -\mathrm{i}\left(1-\dfrac{\lambda k_z}{\omega}\right)J_{j+1}(k_\perp r)\mathrm{e}^{-\mathrm{i}(j+1)\theta} \\ -\mathrm{i}\left(1+\dfrac{\lambda k_z}{\omega}\right)J_{j-1}(k_\perp r)\mathrm{e}^{-\mathrm{i}(j-1)\theta} & -\dfrac{\lambda k_\perp}{\omega}J_j(k_\perp r)\mathrm{e}^{-\mathrm{i}j\theta} \end{bmatrix} \\
&= \begin{bmatrix} -\mathrm{i}\left(1+\dfrac{\lambda k_z}{\omega}\right)S_{j-1}^{m_1+j}|_{n_1=m_1+j} & -\dfrac{\lambda k_\perp}{\omega}S_j^{m_1+j+1}|_{n_1=m_1+j+1} \\ -\dfrac{\lambda k_\perp}{\omega}S_j^{m_1+j-1}|_{n_1=m_1+j-1} & i\left(1-\dfrac{\lambda k_z}{\omega}\right)S_{j+1}^{m_1+j}|_{n_1=m_1+j} \end{bmatrix}.
\end{aligned} \tag{B.35}$$

Ξ_1 can be written as:

$$\begin{aligned}
\Xi_1 &= \big[(E_1+M)\Gamma_1 Q_{p_z,p_\perp} + (p_{1z}\sigma^3\Gamma_1 - \mathrm{i}p_{1\perp}\Gamma_2)(E_p+M)|_{n_2=n_1}, (E_1+M)\Gamma_1(E_p-M)|_{n_2=n_1} \\
&\quad + (p_{1z}\sigma^3\Gamma_1 - \mathrm{i}p_{1\perp}\Gamma_2)Q_{p_z,p_\perp}\big]\cdot\begin{bmatrix} (E_2+M)S_0^{m_2}\delta(m_2-n_2) \\ (p_{2z}\sigma^3)S_0^{m_2}\delta(m_2-n_2) + \mathrm{i}p_{2\perp}\sigma^{\perp\prime\prime} \end{bmatrix} \\
&\quad\times|_{q^0=0,p_z=p_{1z}+k_z,q_z=p_{1z}+k_z-p_{2z},E_p=E_2,n_3=0} \\
&= \begin{bmatrix} A_1\delta_{m_2,m_1+j} & B_1\delta_{m_2,m_1+j+1} \\ C_1\delta_{m_2,m_1+j-1} & D_1\delta_{m_2,m_1+j} \end{bmatrix}.
\end{aligned} \tag{B.36}$$

Similarly, Ξ_2 for S_2 can be obtained:

$$\begin{aligned}
\Xi_2 &= \left[(E_1+M)S_0^{m_1}\delta(m_1-n_5), -p_{1z}S_0^{m_1}\delta(m_1-n_5)\sigma^3 + \mathrm{i}p_{1\perp}\sigma^{\perp\dagger\prime\prime}\right]\cdot \\
&\quad\times\begin{bmatrix} Q_{p_z,p_\perp}(E_2+M)\tilde{\Gamma}_1 + (E_p+M)|_{n_5=n_6}((p_{2z}\sigma^3)\tilde{\Gamma}_1 + \mathrm{i}p_{2\perp}\tilde{\Gamma}_2) \\ -(E_p-M)|_{n_5=n_6}(E_2+M)\tilde{\Gamma}_1 - Q_{p_z,p_\perp}((p_{2z}\sigma^3)\tilde{\Gamma}_1 + \mathrm{i}p_{2\perp}\tilde{\Gamma}_2)\end{bmatrix}. \\
&\quad\times|_{q^0=0,p_z=p_{2z}-k_z,E_p=E_1,q_z=p_{1z}-p_{2z}+k_z,n_4=0} \\
&= \begin{bmatrix} A_2\delta_{m_2,m_1+j} & B_2\delta_{m_2,m_1+j+1} \\ C_2\delta_{m_2,m_1+j-1} & D_2\delta_{m_2,m_1+j} \end{bmatrix}.
\end{aligned} \tag{B.37}$$

At last, we have:

$$\begin{aligned}
S_{fi} &= \frac{-\mathrm{i}Z\mathrm{e}^3}{32\pi^3}\delta(E_1+\omega-E_2)\frac{\sqrt{(E_1-M)(E_2-M)}}{\sqrt{\omega E_1 E_2}}\cdot\int \mathrm{d}p_\perp\, \mathrm{d}q_\perp \frac{p_\perp q_\perp}{(p^2-M^2)\cdot|\vec{p}_1|\cdot|\vec{p}_2|\cdot|\vec{q}|^2}\cdot \\
&\quad\times\xi^{s_1\dagger}\cdot(\Xi_1+\Xi_2)\cdot\xi^{s_2} \\
&= \frac{-\mathrm{i}Z\,\mathrm{e}^3}{32\pi^3}\delta(E_1+\omega-E_2)\frac{1}{|\vec{p_1}||\vec{p_2}|}\sqrt{\frac{(E_1-M)(E_2-M)}{\omega E_1 E_2}}\cdot\xi^{s_1\dagger}(\Sigma_1+\Sigma_2)\xi^{S_2},
\end{aligned} \tag{B.38}$$

where

$$\begin{aligned}
\Xi_1+\Xi_2 &= \begin{bmatrix} A_1\delta_{m_2,m_1+j} & B_1\delta_{m_2,m_1+j+1} \\ C_1\delta_{m_2,m_1+j-1} & D_1\delta_{m_2,m_1+j} \end{bmatrix} + \begin{bmatrix} A_2\delta_{m_2,m_1+j} & B_2\delta_{m_2,m_1+j+1} \\ C_2\delta_{m_2,m_1+j-1} & D_2\delta_{m_2,m_1+j} \end{bmatrix} \\
&= \begin{bmatrix} A\delta_{m_2,m_1+j} & B\delta_{m_2,m_1+j+1} \\ C\delta_{m_2,m_1+j-1} & D\delta_{m_2,m_1+j} \end{bmatrix}.
\end{aligned} \tag{B.39}$$

The coefficients of the four matrix elements are

$$\begin{bmatrix} A & B \\ C & D \end{bmatrix} = \begin{bmatrix} A_1 & B_1 \\ C_1 & D_1 \end{bmatrix}_{q_z=p_z-p_{2z},p_z=p_{1z}+k_z} + \begin{bmatrix} A_2 & B_2 \\ C_2 & D_2 \end{bmatrix}_{q_z=p_{1z}-p_z,p_z=p_{2z}-k_z}, \tag{B.40}$$

$$\begin{aligned} \begin{bmatrix} A_1 & B_1 \\ C_1 & D_1 \end{bmatrix} &= (p_{1z}\sigma^3\Gamma_1 - \mathrm{i}p_{1\perp}\Gamma_2)\left[(E_2+M)^2 S_0^{m_2} + p_{2z}Q\sigma^3 S_0^{m_2} + \mathrm{i}p_{2\perp}QR\right] \\ &\quad + (E_1+M)\Gamma_1[(E_2+M)QS_0^{m_2} + (E_2-M)p_{2z}\sigma^3 S_0^{m_2} + \mathrm{i}p_{2\perp}(E_2-M)R], \end{aligned} \tag{B.41}$$

$$\begin{aligned} \begin{bmatrix} A_2 & B_2 \\ C_2 & D_2 \end{bmatrix} &= (E_1+M)S_0^{m_1}[(E_1+M)(p_{2z}\tilde{\Gamma}_1\sigma^3 + \mathrm{i}p_{2\perp}\tilde{\Gamma}_2) - (E_2+M)\tilde{\Gamma}_1 Q] \\ &\quad - p_{1z}\sigma^3 S_0^{m_1} Q(p_{2z}\tilde{\Gamma}_1\sigma^3 + \mathrm{i}p_{2\perp}\tilde{\Gamma}_2) + p_{1z}\sigma^3 S_0^{m_1}\tilde{\Gamma}_1(E_2+M)(E_1-M) \\ &\quad + \mathrm{i}p_{1\perp}\tilde{R}Q(p_{2z}\tilde{\Gamma}_1\sigma^3 + \mathrm{i}p_{2\perp}\tilde{\Gamma}_2) - \mathrm{i}p_{1\perp}\tilde{R}\tilde{\Gamma}_1(E_2+M)(E_1-M), \end{aligned} \tag{B.42}$$

where

$$S_0^{m_1} = S_0^{m_1}(q_\perp, p_{1\perp}, p_\perp), \tag{B.43}$$

$$S_0^{m_2} = S_0^{m_2}(q_\perp, p_{2\perp}, p_\perp), \tag{B.44}$$

$$\sigma^3 = \begin{bmatrix} 1 & 0 \\ 0 & -1 \end{bmatrix}, \tag{B.45}$$

$$Q = \begin{bmatrix} p_z & -\mathrm{i}p_\perp \\ \mathrm{i}p_\perp & -p_z \end{bmatrix}, \tag{B.46}$$

$$R = \begin{bmatrix} 0 & -S_0^{m_2-1}(q_\perp, p_{2\perp}, p_\perp) \\ S_0^{m_2+1}(q_\perp, p_{2\perp}, p_\perp) & 0 \end{bmatrix}, \tag{B.47}$$

$$\tilde{R} = \begin{bmatrix} 0 & S_0^{m_1+1}(q_\perp, p_{1\perp}, p_\perp) \\ -S_0^{m_1-1}(q_\perp, p_{1\perp}, p_\perp) & 0 \end{bmatrix}, \tag{B.48}$$

$$\Gamma_1 = \begin{bmatrix} \frac{\lambda k_\perp}{\omega} S_j^{m_1+j}(k_\perp, p_\perp, p_{1\perp}) & \mathrm{i}\left(-1+\frac{\lambda k_z}{\omega}\right) S_{j+1}^{m_1+j+1}(k_\perp, p_\perp, p_{1\perp}) \\ \mathrm{i}\left(-1-\frac{\lambda k_z}{\omega}\right) S_{j-1}^{m_1+j-1}(k_\perp, p_\perp, p_{1\perp}) & -\frac{\lambda k_\perp}{\omega} S_j^{m_1+j}(k_\perp, p_\perp, p_{1\perp}) \end{bmatrix}, \tag{B.49}$$

$$\Gamma_2 = \begin{bmatrix} \mathrm{i}\left(-1-\frac{\lambda k_z}{\omega}\right) S_{j-1}^{m_1+j}(k_\perp, p_\perp, p_{1\perp}) & -\frac{\lambda k_\perp}{\omega} S_j^{m_1+j+1}(k_\perp, p_\perp, p_{1\perp}) \\ -\frac{\lambda k_\perp}{\omega} S_j^{m_1+j-1}(k_\perp, p_\perp, p_{1\perp}) & \mathrm{i}\left(1-\frac{\lambda k_z}{\omega}\right) S_{j+1}^{m_1+j}(k_\perp, p_\perp, p_{1\perp}) \end{bmatrix}. \tag{B.50}$$

$$\tilde{\Gamma}_1 = \begin{bmatrix} \frac{\lambda k_\perp}{\omega} S_j^{m_2}(k_\perp, p_{2\perp}, p_\perp) & \mathrm{i}\left(-1+\frac{\lambda k_z}{\omega}\right) S_{j+1}^{m_2}(k_\perp, p_{2\perp}, p_\perp) \\ \mathrm{i}\left(-1-\frac{\lambda k_z}{\omega}\right) S_{j-1}^{m_2}(k_\perp, p_{2\perp}, p_\perp) & -\frac{\lambda k_\perp}{\omega} S_j^{m_2}(k_\perp, p_{2\perp}, p_\perp) \end{bmatrix}, \tag{B.51}$$

$$\tilde{\Gamma}_2 = \begin{bmatrix} \mathrm{i}\left(-1+\frac{\lambda k_z}{\omega}\right) S_{j+1}^{m_2+1}(k_\perp, p_{2\perp}, p_\perp) & -\frac{\lambda k_\perp}{\omega} S_j^{m_2-1}(k_\perp, p_{2\perp}, p_\perp) \\ -\frac{\lambda k_\perp}{\omega} S_j^{m_2+1}(k_\perp, p_{2\perp}, p_\perp) & \mathrm{i}\left(1+\frac{\lambda k_z}{\omega}\right) S_{j-1}^{m_2-1}(k_\perp, p_{2\perp}, p_\perp) \end{bmatrix}. \tag{B.52}$$

Appendix C. Derivation of vortex electron wave function with impact parameter b

$$
\begin{aligned}
\psi^{s_2}_{p_2,m_2}(x,\vec{b}) &= \int \tilde{\psi}_{m_2}(\vec{p'})\psi(x)\mathrm{e}^{-\mathrm{i}\vec{p'}_\perp\cdot\vec{b}}p'_\perp \mathrm{d}p'_\perp\,\mathrm{d}\phi_{p'}\,\mathrm{d}p'_z \\
&= \frac{1}{\sqrt{2\pi}i^{m_2}p_{2\perp}}\int \delta(p'_\perp - p_{2\perp})\delta(p'_z - p_{2z})\mathrm{e}^{\mathrm{i}m_2\phi_{p'}}u(\vec{p'})\mathrm{e}^{\mathrm{i}\vec{p'}\cdot\vec{x}-\vec{p'}_\perp\cdot\vec{b}-\mathrm{i}E_2t}p'_\perp\mathrm{d}p'_\perp\mathrm{d}\phi_{p'}\,\mathrm{d}p'_z \\
&= \frac{\mathrm{e}^{\mathrm{i}p_{2z}z-\mathrm{i}E_2t}}{\sqrt{2\pi}\mathrm{i}^{m_2}p_{2\perp}}\int u(\vec{p'})\mathrm{e}^{\mathrm{i}p'_\perp r\,\cos(\phi_{p'}-\theta)-\mathrm{i}p'_\perp b\,\cos(\phi_{p'}-\theta_b)+\mathrm{i}m_2\phi_{p'}}\delta(p'_\perp - p_{2\perp})p'_\perp\mathrm{d}p'_\perp\,\mathrm{d}\phi_{p'} \\
&= \frac{\mathrm{e}^{\mathrm{i}p_{2z}z-\mathrm{i}E_2t}}{\sqrt{2}(2\pi)^2\mathrm{i}^{m_2}}\int\left(\begin{bmatrix}\sqrt{1+\frac{M}{E_2}}\xi^{s_2}\\ \sqrt{1-\frac{M}{E_2}}\frac{p_{2z}}{|\vec{p}_2|}\sigma^3\xi^{s_2}\end{bmatrix}+\left[\sqrt{1-\frac{M}{E_2}}\frac{p_{2\perp}}{|\vec{p}_2|}\begin{bmatrix}0 & \mathrm{e}^{-\mathrm{i}\phi_{p'}}\\ \mathrm{e}^{\mathrm{i}\phi_{p'}} & 0\end{bmatrix}\xi^{s_2}\right]\right) \\
&\quad\cdot\mathrm{e}^{\mathrm{i}p_{2\perp}r\,\cos(\phi_{p'}-\theta)-\mathrm{i}p_{2\perp}b\,\cos(\phi_{p'}-\theta_b)+\mathrm{i}m_2\phi_{p'}}\mathrm{d}\phi_{p'} \\
&= \frac{\mathrm{e}^{\mathrm{i}p_{2z}z-\mathrm{i}E_2t}}{\sqrt{2}(2\pi)^2\mathrm{i}^{m_2}}\sum_n\int\left(\begin{bmatrix}\sqrt{1+\frac{M}{E_2}}\xi^{s_2}\\ \sqrt{1-\frac{M}{E_2}}\frac{p_{2z}}{|\vec{p}_2|}\sigma^3\xi^{s_2}\end{bmatrix}+\left[\sqrt{1-\frac{M}{E_2}}\frac{p_{2\perp}}{|\vec{p}_2|}\begin{bmatrix}0 & \mathrm{e}^{-\mathrm{i}\phi_{p'}}\\ \mathrm{e}^{\mathrm{i}\phi_{p'}} & 0\end{bmatrix}\xi^{s_2}\right]\right) \\
&\quad\cdot\mathrm{i}^{-n}J_n(p_{2\perp}b)\mathrm{e}^{-\mathrm{i}n\theta_b+\mathrm{i}n\phi_{p'}}\mathrm{e}^{\mathrm{i}p_{2\perp}r\,\cos(\phi_{p'}-\theta)+\mathrm{i}m_2\phi_{p'}}\mathrm{d}\phi_{p'} \\
&= \frac{\mathrm{e}^{\mathrm{i}p_{2z}z-\mathrm{i}E_2t}}{\sqrt{2}(2\pi)^2\mathrm{i}^{m_2}}\sum_n\mathrm{i}^{-n}\,\mathrm{e}^{-\mathrm{i}n\theta_b}J_n(p_{2\perp}b)\int\left(\begin{bmatrix}\sqrt{1+\frac{M}{E_2}}\xi^{s_2}\\ \sqrt{1-\frac{M}{E_2}}\frac{p_{2z}}{|\vec{p}_2|}\sigma^3\xi^{s_2}\end{bmatrix}\mathrm{e}^{\mathrm{i}(m_2+n)\phi_{p'}}\right. \\
&\quad\left.+\left[\sqrt{1-\frac{M}{E_2}}\frac{p_{2\perp}}{|\vec{p}_2|}\begin{bmatrix}0 & \mathrm{e}^{\mathrm{i}(m_2+n-1)\phi_{p'}}\\ \mathrm{e}^{\mathrm{i}(m_2+n+1)\phi_{p'}} & 0\end{bmatrix}\xi^{s_2}\right]\right)\cdot\mathrm{e}^{\mathrm{i}p_{2\perp}r\,\cos(\phi_{p'}-\theta)}\mathrm{d}\phi_{p'} \\
&= \frac{\mathrm{e}^{\mathrm{i}p_{2z}z-\mathrm{i}E_2t}}{\sqrt{2}(2\pi)}\sum_n\mathrm{e}^{-\mathrm{i}n\theta_b}J_n(p_{2\perp}b)\cdot\left(\begin{bmatrix}\sqrt{1+\frac{M}{E_2}}\xi^{s_2}\\ \sqrt{1-\frac{M}{E_2}}\frac{p_{2z}}{|\vec{p}_2|}\sigma^3\xi^{s_2}\end{bmatrix}J_{m_2+n}(p_{2\perp}r)\mathrm{e}^{\mathrm{i}(m_2+n)\theta}\right. \\
&\quad\left.+\frac{\mathrm{i}p_{2\perp}}{|\vec{p}_2|}\sqrt{1-\frac{M}{E_2}}\left[\begin{bmatrix}0 & 0\\ J_{m_2+n+1}(p_{2\perp}r)\mathrm{e}^{\mathrm{i}(m_2+n+1)\theta} & -J_{m_2+n-1}(p_{2\perp}r)\mathrm{e}^{\mathrm{i}(m_2+n-1)\theta}\\ & 0\end{bmatrix}\xi^{s_2}\right]\right) \\
&= \sum_n\mathrm{e}^{-\mathrm{i}n\theta_b}J_n(p_{2\perp}b)\cdot\psi^{s_2}_{p_2,m'_2}(x)|_{m'_2=m_2+n}. \qquad \text{(C.1)}
\end{aligned}
$$

ORCID iDs

W Q Wang https://orcid.org/0000-0001-5659-0714
X S Geng https://orcid.org/0000-0003-1181-6518
B F Shen https://orcid.org/0000-0003-1021-6991
L L Ji https://orcid.org/0000-0002-7107-0626

References

[1] Allen L, Beijersbergen M W, Spreeuw R J C and Woerdman J P 1992 *Phys. Rev.* A **45** 8185–9
[2] Karlovets D V 2012 *Phys. Rev.* A **86** 062102
[3] Bliokh K Y, Bliokh Y P, Savel'ev S and Nori F 2007 *Phys. Rev. Lett.* **99** 190404
[4] Bliokh K Y and Nori F 2012 *Phys. Rev.* A **86** 033824
[5] Bliokh K Y, Dennis M R and Nori F 2017 *Phys. Rev.* A **96** 023622
[6] Bliokh K Y, Schattschneider P, Verbeeck J and Nori F 2012 *Phys. Rev.* X **2** 041011
[7] Schattschneider P, Schachinger T, Stöger-Pollach M, Löffler S, Steiger-Thirsfeld A, Bliokh K Y and Nori F 2014 *Nat. Commun.* **5** 4586

[8] Guzzinati G, Schattschneider P, Bliokh K Y, Nori F and Verbeeck J 2013 *Phys. Rev. Lett.* **110** 093601
[9] Karlovets D V, Kotkin G L, Serbo V G and Surzhykov A 2017 *Phys. Rev.* A **95** 032703
[10] Karlovets D V and Pupasov-Maksimov A M 2021 *Phys. Rev.* A **103** 012214
[11] Karlovets D V and Serbo V G 2020 *Phys. Rev.* D **101** 076009
[12] Karlovets D 2019 *Phys. Rev.* A **99** 043824
[13] Karlovets D 2018 *Phys. Rev.* A **98** 012137
[14] Sherwin J A 2018 *Phys. Rev.* A **98** 042108
[15] Sherwin J A 2020 *Phys. Rev. Res.* **2** 013168
[16] Beijersbergen M W, Coerwinkel R P C, Kristensen M and Woerdman J P 1994 *Opt. Commun.* **112** 321–7
[17] Turnbull G A, Robertson D A, Smith G M, Allen L and Padgett M J 1996 *Opt. Commun.* **127** 183–8
[18] Oemrawsingh S S R, van Houwelingen J A W, Eliel E R, Woerdman J P, Verstegen E J K, Kloosterboer J G and 't Hooft G W 2004 *Appl. Opt.* **43** 688–94
[19] Sueda K, Miyaji G, Miyanaga N and Nakatsuka M 2004 *Opt. Express* **12** 3548–53
[20] Uchida M and Tonomura A 2010 *Nature* **464** 737–9
[21] Verbeeck J, Tian H and Schattschneider P 2010 *Nature* **467** 301–4
[22] McMorran B J, Agrawal A, Anderson I M, Herzing A A, Lezec H J, McClelland J J and Unguris J 2011 *Science* **331** 192–5
[23] Yao A M and Padgett M J 2011 *Adv. Opt. Photon.* **3** 161–204
[24] Pupasov-Maksimov A and Karlovets D 2021 *New J. Phys.* **23** 043011
[25] Bogdanov O V, Kazinski P O, Korolev P S and Lazarenko G Y 2021 *Phys. Rev.* E **104** 024701
[26] Bogdanov O V, Kazinski P O, Korolev P S and Lazarenko G Y 2021 *J. Mol. Liq.* **326** 115278
[27] Bogdanov O V, Kazinski P O and Lazarenko G Y 2020 *Ann. Phys.* **415** 168116
[28] Bogdanov O V and Kazinski P O 2019 *Eur. Phys. J. Plus* **134** 586
[29] Bogdanov O V, Kazinski P O and Lazarenko G Y 2020 *J. Inst.* **15** C04008
[30] Bogdanov O V, Kazinski P O and Lazarenko G Y 2020 *Eur. Phys. J. Plus* **135** 901
[31] Kazinski P O and Ryakin V A 2021 *Russ. Phys. J.* **64** 717–27
[32] Serbo V G, Surzhykov A and Volotka A 2021 *Ann. Phys.* **534** 2100199
[33] Karlovets D V, Serbo V G and Surzhykov A 2021 *Phys. Rev.* A **104** 023101
[34] Bliokh K Y *et al* 2017 *Phys. Rep.* **690** 1–70
[35] Ivanov I P 2011 *Phys. Rev.* D **83** 093001
[36] Seipt D, Surzhykov A and Fritzsche S 2014 *Phys. Rev.* A **90** 012118
[37] Serbo V, Ivanov I P, Fritzsche S, Seipt D and Surzhykov A 2015 *Phys. Rev.* A **92** 012705
[38] Groshev M E, Zaytsev V A, Yerokhin V A and Shabaev V M 2020 *Phys. Rev.* A **101** 012708
[39] Ivanov I P 2012 *Phys. Rev.* D **85** 076001
[40] Ivanov I P, Seipt D, Surzhykov A and Fritzsche S 2016 *Europhys. Lett.* **115** 41001
[41] Ivanov I P, Seipt D, Surzhykov A and Fritzsche S 2016 *Phys. Rev.* D **94** 076001
[42] Karlovets D 2016 *Europhys. Lett.* **116** 31001
[43] Karlovets D V 2017 *J. High Energy Phys.* JHEP03(2017)049
[44] Ivanov I P 2012 *Few-Body Syst.* **53** 167–72
[45] Ivanov I P 2013 *AIP Conf. Proc.* **1523** 128–31
[46] Jentschura U D and Serbo V G 2011 *Phys. Rev. Lett.* **106** 013001
[47] Jentschura U D and Serbo V G 2011 *Eur. Phys. J.* C **71** 1571
[48] Ivanov I P and Serbo V G 2011 *Phys. Rev.* A **84** 033804
[49] Ivanov I P 2012 *Phys. Rev.* A **85** 033813
[50] Bliokh K Y, Dennis M R and Nori F 2011 *Phys. Rev. Lett.* **107** 174802